2015

Nitric Oxide Synthase Activity and its Modulation in the Treatment of Colorectal Cancer

Asim Alam
Virginia Commonwealth University, alama4@vcu.edu

Nitric Oxide Synthase Activity and its Modulation in the Treatment of Colorectal Cancer

A dissertation submitted in partial fulfillment of the requirements for the degree of Doctor of Philosophy at Virginia Commonwealth University.

by

Asim Alam

Bachelor of Science, University of California, San Diego 2008

Ross B. Mikkelsen, PhD

Professor and Vice Chair for Research, Department of Radiation Oncology

Virginia Commonwealth University

Richmond, Virginia

December 2, 2015

Acknowledgements

First and foremost, I'd like to thank God for all the blessings I have received in life and to finally finish my dissertation work!

There are a number of individuals who have helped me so far on this journey, none more important than my parents Muzaffar and Shakra Alam. Thank you for always supporting us and giving us the opportunity to study and grow up in America. Hopefully your sacrifices were worth it. To my brothers Arfeen and Omair and sisters Mahza, Nisa and Hiba, thank you for being my best friends through all of my time growing up and now… and for leaving California for Richmond so we could be closer.

Thank you to my wife, Zayneb, who luckily for her hasn't had to deal with my whole PhD experience, but has made this past year very easy for me to finish. Thank you for being understanding and loving especially when I am being difficult. I am eternally gratefully to have met you.

The past and present members of the Mikkelsen Lab: Drs. Robert Cardnell, Eric Howlett, Vasily Yakovlev, Chris Rabender and Master's candidate Ninu Bruno. Thank you all for your support in teaching me techniques and answering my usually rudimentary questions. I am indebted to you all for all I have learned in the Mikkelsen Lab. Thank you also for being friends and keeping the lab a more friendly and social environment.

Dr. Mikkelsen, thank you for being a very caring and motivating advisor. Thank you for letting me venture on my own with my projects, for discussing topics with me as an equal and for accepting me into the MD/PhD program. We have not seen eye to eye on everything, but I appreciate how understanding you have been with me as a student and person. You truly do care for the people in the lab more than just students or workers, but for us as individuals.

A number of people have been instrumental in helping me finish my project: Dr. Gobalakrishna, Li Wang and Reed McDonagh from Dr. Zweit's lab for FDG/PET imaging and AOM/DSS animal care. Jason Beckta and Valerie Lab members for materials support and confocal imaging. Justin Sperlazza from Dr. Ginder's Lab for help with lentiviral transfection and qPCR techniques. Mike Waters from Dr. Kordula lab for TCGA data acquisition and analysis.

Dr. Archer (retired), Sandra Sorrell and the MD/PhD program for giving me the opportunity to acquire both degrees. Thank you for taking a chance on me.

Table of Contents

Page

ABBRREVIATIONS

AOM	azoxymethane
APC	adenomatous polyposis coli
BH2	dihydrobiopterin
BH4	tetrahydrobiopterin
CAC	Colitis associated Colorectal Cancer
cGMP	3,5 cyclic guanine monophosphate
COX	Cyclooxygenase
CRC	Colorectal Cancer
DHFR	Dihydrofolate Reductase
DSS	Dextran Sodium Sulfate
EGFR	Epidermal Growth Factor Receptor
eNOS	endothelial Nitric Oxide Synthase
ERK 1/2	Extracellular Regulated Kinase
FAP	Familial Adenomatous Polyposis
FBS	Fetal Bovine Serrum
[^{18}F]-FDG	Fluorine-18-fluorodeoxyglucose
GCH-1	GTP cyclohydrolase I
GFRP	GCH-1 Feedback Regulating Protein
GSK3	Glycogen Synthase Kinase 3
GSNO	S Nitrosoglutathione
GTP	Guanosine triphosphate
HIF	Hypoxia Inducible Factor

HPLC	High Performance Liquid Chromatography
IBD	Inflammatory Bowel Disease
i.p.	intraperitoneal
IF	Immunofluorescence
IHC	Immunohistochemical
iNOS	inducible Nitric Oxide Synthase
IP	immunoprecipitate
IκB	Inhibitor of kappa B
JAK	Janus Kinases
L-NAME	N-Nitro-L-Arginine Methyl Ester
L-NNA	NG-nitro-L-Arginine
Luc	Luciferase
MAPK	Mitogen Activated Protein Kinase
MMP-7	Matrix metalloprotein-7
MMTS	methylmethanethiosulfonate
MTX	Methotrexate
NADPH	Nicotinamide Adenine dinucleotide phosphate-reduced
NFκB	Nuclear Factor kappa B
nNOS	neuronal Nitric Oxide Synthase
NO	Nitric Oxide
NOS	Nitric Oxide Synthase
NSAID	Non-Steroidal Anti-Inflammatory Drugs
O_2^-	Superoxide

$ONOO^-$	Peroxynitrite
PDE	Phosphodiesterase
Pen Step	Penicillin Streptomycin
PET	Positron Emitted Topography
PKG	cGMP dependent protein kinase
PTP	Protein Tyrosine Phosphatase
QDPR	Quinone Dihydropteridine Reductase
RNS	Reactive Nitrogen Species
ROR	Retinoid-related orphan receptor
ROS	Reactive Oxygen Species
SDS-Page	Sodium Dodecyl Sulfate Polyacrylamide Gel Electrophoresis
sGC	soluble guanylyl cyclase
SOD	Superoxide Dismutase
SP	Sepiapterin
SPR or SR	Sepiapterin Reductase
STAT	Signal Transducer and Activator of Transcription
TAM	Tumor associated macrophage
TGFβ	Transforming growth factor β
TNF	Tumor Necrosis Factor
T_{reg}	Regulatory T Cells
VEGF	Vascular endothelial growth factor

Abstract

The American Cancer Society estimates more than 141,000 new cases of and about 50,000 deaths from colorectal cancer every year. Treatment options include surgery, radiation therapy and targeted therapies such as anti-angiogenics. However, no therapies address the key driving factor of colorectal cancer: inflammation. It is well known that chronic inflammatory conditions such as Crohn's Disease, ulcerative colitis, diabetes, obesity and cigarette smoking all elevate the risk of developing colorectal cancer. One of the hallmarks of chronic inflammation is the elevated levels of reactive oxygen/nitrogen species (ROS/RNS). A primary source of these ROS/RNS is uncoupled Nitric Oxide Synthase (NOS). Under non-inflammatory conditions NOS generates Nitric Oxide. However, in an inflammatory environment, such as the oxidative tumor microenvironment, NOS's cofactor tetrahydrobiopterin (BH4) is oxidized to dihydrobiopterin (BH2). NOS bound to BH2 is said to be uncoupled and produces superoxide O_2^- and peroxynitrite ($ONOO^-$). Previous work in our and other's labs have shown that increased production of ROS/RNS leads to the activation of pro-inflammatory/proliferative molecules such as NFκB, Stat3, β-Catenin and Akt. NOS can be re-coupled by supplementing cells and animals with BH4 or its precursor Sepiapterin (SP). Herein we show that recoupling NOS with SP in HCT116, Caco-2 and HT29 cells, decreased tumor cell proliferation, increased β-Catenin degradation and decreased Akt activity. We also see increased tumor cell death measured by *in vitro* clonogenic assay, as well as decreased metabolic uptake in Azoxymethane/Dextran Sodium Sulfate (AOM/DSS) induced colorectal cancer *in vivo* measured by [^{18}F]-fluorodeoxyglucose ([^{18}F]-FDG) positron emitted topography (PET) imaging. We believe by recoupling NOS both *in vivo* and *in vitro* we are modulating Wnt signaling via Akt and GSK-

3β. Lastly, we conducted studies to determine a mechanistic explanation of how tumor cells maintain a decreased BH4:BH2 ratio.

Chapter 1: Introduction

Background and Significance

Colorectal Cancer and Inflammation

The American Cancer Society estimates that there are more than 141,000 new cases and about 50,000 deaths from colorectal cancer (CRC) every year in the U.S. CRC is the third leading cause of cancer-related deaths in both men and women with 1 in 20 Americans developing colorectal cancer in their lifetimes [1]. The 5 year survival rate for lesions discovered in early stages is greater than 70%, however for advanced or metastatic lesions the 5 year survival drops to less than 11%. Although the incidence and mortality rates have been slowly but steadily declining due to better screening guidelines, colorectal cancer is still a disease with significant mortality and morbidity [1]. Elucidation of the genetic and molecular mechanisms of colorectal tumor development coupled with increased screening has, in part, played a role in the decline of incidence and our understanding of tumor initiation. However, more research is needed to understand the progression and maintenance of colorectal cancer and for the development of new treatment options.

Many factors have been identified which increase the risk of developing colorectal cancer. Thus far, age has been shown to be the greatest risk factor of developing sporadic colorectal tumors [2]. Other risk factors include obesity, cigarette use, diet and inflammatory bowel diseases such as Ulcerative Colitis and Crohn's Disease [3]. Although inherited genetic mutations such as those found in Familial Adenomatous Polyposis (FAP) and hereditary nonpolyposis colorectal cancer (HNCC) confer a 90 percent chance of developing tumors, combined these inherited genetic disorders account for only about 5% of CRC [4-6]. However the genetic alterations found in FAP and HNCC have been invaluable tools to elucidate the mechanisms of tumor initiation and progression in colorectal cancer.

Patients with FAP disease have a germline mutation in one copy of the tumor suppressor gene, Adenomatous Polyposis Coli (*APC)*. The second copy of the gene is typically mutated within the first 30 years of life resulting in multiple tumors [7]. APC is an inhibitor of β-catenin, the effector molecule which activates Wnt signaling. The Wnt signal pathways regulate cell adhesion, migration, apoptosis and chromosome segregation during mitosis [8]. Most sporadic tumors have somatic mutations in *APC* gene as well. The cascade of mutations and histopathological changes have been well characterized by the work of Drs. Vogelstein and Kinzler [9-12], summarized below. Mutations in the *APC* gene have been shown to occur at the earliest stage of carcinoma development, the aberrant crypt foci. Two hits to the *APC* gene are required for loss of function providing the mutated cells a selective advantage to grow clonally. The oncogene *KRAS* is mutated next. Interestingly, *KRAS* is also mutated in about 50% of sporadic CRC. The combination of loss of *APC* and activating mutation in *KRAS* leads

to clonal expansion and dysplasia, histologically termed an adenoma. It is postulated that other unknown oncogenes are also mutated in the subset of CRC tumors which do not show *KRAS* mutations to allow for adenoma formation. As the adenoma progresses to adenocarcinoma, further mutations in *TP53* and *SMAD2* and *SMAD4* tumor suppressor genes appear [10, 13, 14]. *TP53* mutations arise in greater than 75% of spontaneous CRC, however rarely in the benign early stages of disease. p53 is an important regulator of DNA damage repair and cell cycle regulation [15]. SMAD2/4 are transcription factors activated by TGF-β signaling. In colorectal epithelial cells TGF-β signaling is thought to inhibit growth and promote differentiation of these cells [16, 17]. This genetic model developed by Vogelstein and colleagues predicts a minimum of 7 genetic mutations to initiate a polyp and progress to carcinoma stage [9].

Wnt signaling is a critical regulator of normal cell turn over in healthy colonic epithelial cells. However, in over 90% of spontaneous CRC activation mutations in Wnt signaling have been found in the early stages of development leading to malignancy. The major effector of Wnt signaling is β-Catenin. β-Catenin is an important regulator of cell growth in normal and malignant colonic epithelial cells. The most common activating mutation of Wnt signaling is in APC. In the absence of Wnt ligand, APC binds to phosphorylated β-Catenin (Serine 33/39) and forms the destruction complex. β-Catenin is ubiquitinated and subsequently degraded by the proteasome complex [18] (Figure 1.1). Other activating mutations of Wnt pathway can be loss of function of Glycogen Synthase Kinase-3β (GSK-3β), which is the kinase responsible for β-Catenin phosphorylation at Serine 33/39, constitutive activation of Wnt receptor absent of any ligand as well as mutated forms of β-Catenin which are unable to bind APC protein [19].

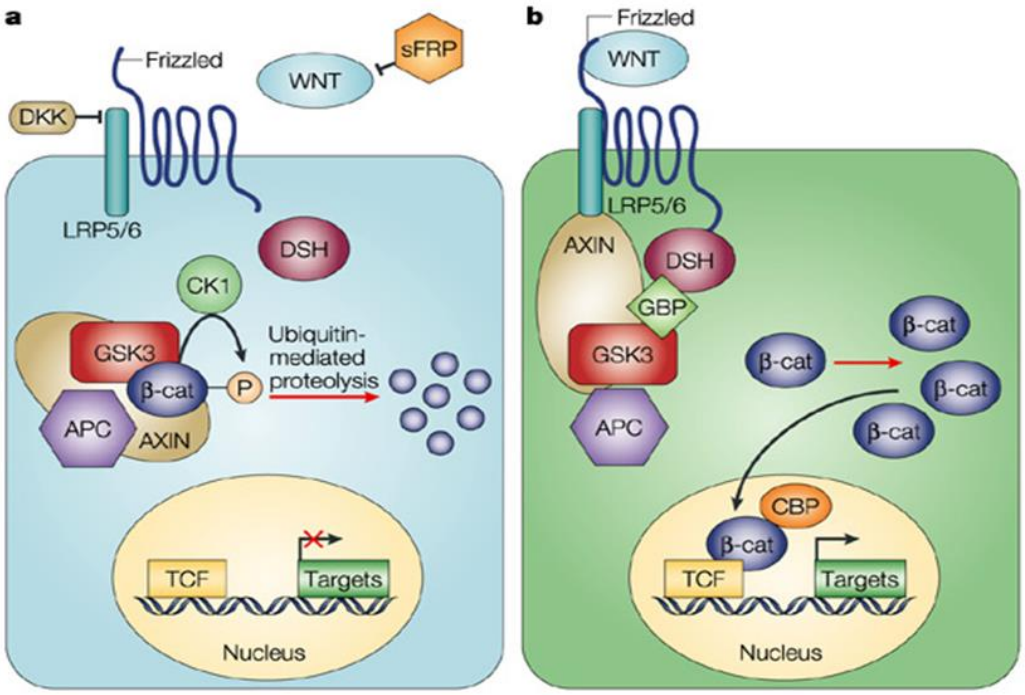

Figure 1.1: Canonical Wnt Signaling. (a) Absent Ligand, β-catenin remains in complex with APC and GSK3β resulting in its phosphorylation and subsequent degradation. (b) Ligand bound receptor results in inhibition of GSK3β and β-catenin is then able to accumulate and move into nucleus, activating transcription of targeted genes. Figure provided by Nature Reviews, Moon 2004.

The end result of aberrant Wnt signaling is nuclear accumulation of β-Catenin. Cooperating with members of the TCF/LEF family, β-catenin activates a number of target genes such as cyclin D1, claudin-1, VEGF and MMP-7, which modulate cell proliferation, metastasis and further progression of tumors [8]. Increasing amounts of evidence points to a profound effect of inflammation driving further changes in morphology, genetic mutations and molecular changes within the tumor and its microenvironment as the tumor progresses.

Inflammatory bowel diseases (IBD) such as Ulcerative colitis and Crohn's Disease are characterized by colitis of the large intestine. Patients with these diseases have between a 5 and15 fold increased risk of developing cancer in their lifetimes. The tumors arising in these patients are difficult to treat and have a >50% mortality rate [20-22]. The histopathology of Colitis Associated Cancer (CAC) is very similar to hereditary or sporadic CRC, and the same genetic mutations are found within these different tumors. A key component in both of these etiologies of CRC is the increased nuclear accumulation of β-Catenin. However, the timing of mutations is different: CAC tumors display earlier p53 mutations and later Kras mutations, whereas sporadic CRC tumors show earlier APC mutations and Kras mutations, with p53 mutations generally arising later, as the tumor progresses [22, 23]. This is the case in both mouse models of tumors and human tumors. Perhaps inflammation leads to or is a prerequisite of p53 mutation. Many groups have shown substantial inflammatory markers increased in CRC. There is growing evidence showing robust pro-inflammatory infiltrates as well as increased pro-inflammatory cytokine levels in CRC without any clinically detectable signs of gastrointestinal distress [19]. Moreover, patients with IBD and a family history of CRC

are twice as likely to develop cancer, compared to IBD patients without a positive family history [24]. Thus there could be a mechanistic overlap and a dependence on inflammation, even in hereditary or sporadic CRC. More evidence for inflammation being a driver for both sporadic CRC and CAC is the clinical observation that Non-steroidal Anti-inflammatory Drugs (NSAIDs) such as aspirin confer protection from tumor development [25-27].

Several bodies of evidence have implicated the tumor cells and infiltrating immune cells of the colon for the increase in inflammation and the resulting addiction of the tumor cells to inflammation. CRC tumors and cell lines show constitutive activation of transcription factors that are integral molecules of multiple key inflammatory pathways, such as Nuclear Factor-κB (NF-κB) and Signal Transducer and Activator of Transcription 3 (STAT3) [28, 29]. β-Catenin alters the anti-tumorigenic function of Regulatory-T cells (Tregs) into pro-tumorigenic via increased expression of RORγt receptor, which leads to increased inflammatory cytokines [30]. The inflammatory environment itself can increase β-catenin nuclear accumulation. For instance, it has been shown that TNFα derived from tumor associated macrophages (TAM) in gastric cancers can cause the nuclear accumulation of β-catenin in tumor cells [31, 32]. Activated macrophages also secrete IL-1β, which stimulates Wnt signaling in CRC cells [33]. Thus, the combination of these events (which would occur in both sporadic CRC and CAC) lead to an inflammatory microenvironment. This inflammatory environment is integral to tumor progression because it allows for further accumulation of mutations, promotes maintenance and progression to metastasis in the tumor cells.

Nitric Oxide Synthase Modulation in Inflammation

A hallmark for an inflammatory microenvironment is the increase in reactive oxygen/nitrogen species (ROS/RNS) leading to an oxidative state in the cell. One of the primary sources of ROS/RNS is Nitric Oxide Synthase (NOS). There are 3 subtypes of NOSs: neuronal (nNOS, NOSI), inducible (iNOS, NOS II) and endothelial (eNOS, NOS III) which catalyze the production of nitric oxide (NO) and L-citrulline by the oxidation of L-arginine [34]. NOS forms homodimers and uses arginine and molecular oxygen (O_2) as substrates. Tetrahydrobiopterin (BH4), NADPH, FAD and FMN are all required as cofactors [35]. Both NOS I and NOS III are constitutively expressed in neural cells and endothelial cells respectively and are responsible for a low basal level of NO synthesis. NOS III is membrane associated and is constitutively expressed in endothelial cells and cardiac myocytes and is involved in maintaining vascular tone, platelet aggregation, angiogenesis and smooth muscle cell proliferation. The NOS II and III isoforms are expressed in a variety of tumor cells [36-38] and for this reason will be the main focus in the studies in this dissertation. NOS I is constitutively expressed in neurons and acts as a neurotransmitter in both the central and peripheral nervous system. In skeletal muscle NOS I is responsible for producing large amounts of NO during contraction [39]. NOS II is found in a variety of cell types including fibroblasts, macrophages, dendritic cells, epithelial cells, and some cancer cells. NOS II plays a role in host immunity and upon induction produces 100x more NO than NOS I & III. This burst in NO in an inflammatory environment can react with O_2^- leading to cell toxicity [40].

Under normal physiological conditions NOS produces NO via the reaction mentioned above. The heme moiety of soluble guanylate cyclase (sGC) is the main

relevant target of NO at physiological concentrations produced by NOSI and NOSIII. NO binding to the heme of sGC leads to the formation of 3,5-cyclic guanylate monophosphate (cGMP) from guanosine triphosphate (GTP). cGMP is the principle messenger involved in vasodilation, neurotransmission and platelet aggregation. NO is the primary vasoregulator in mammalian cells and the generation of cGMP results in the subsequent activation of cGMP dependent protein kinase (PKG) leading to the phosphorylation of vasodilator-stimulated phosphoprotein (VASP) and the inositol 1,4,5-triphosphate receptor (IP3 receptor) resulting in vasodilation [41]. New evidence shows, in tumors cells, activation of PKG to be anti-proliferative and pro-apoptotic [42-44]. Thus there is an apparent disconnect between expression of NOSIII and NOSII [37, 38, 45, 46] and NOS activity in tumor cells and the experimentally observed anti-tumor properties of NO. Since NOS is expressed in tumor cells, NO should signal towards anti-proliferative and apoptotic pathways. However this is not the case, tumors continue to grow and progress. Previous work in our lab, as well as the studies in this thesis seek explanations for this phenomenon.

One explanation is that NOSs in tumor cells do not synthesize NO. Under normal, non-inflammatory/non-oxidative states, NOS is said to be coupled with oxidation of arginine resulting in the synthesis of citrulline and NO. However under inflammatory or oxidative conditions, catalytic cycle of NOS is uncoupled and instead of NO, superoxide is formed and NOS is said to be uncoupled. The molecule responsible for determining the coupled state is BH4, and the ratio with its oxidized counterpart dihydrobiopterin (BH2) [47]. Much of this work was first demonstrated in cardiac tissue during myocardial infarctions. In normal non-ischemic tissue NOS is coupled and

predominantly produces NO. The BH4:BH2 is high, thus an abundance of BH4. However, after an infarct the resulting ischemia and an enhanced oxidative state of the tissue cause the oxidation of BH4 to BH2, resulting in a drop of BH4:BH2 ratio. Both BH4 and BH2 have equal affinity for NOS, the relative abundance of either molecule determines the coupling state of NOS [48-50] (Figure 1.2). Because in either state, both BH4 and BH2 are present, there is always a pool of NO producing NOS and O_2^- producing NOS (allowing for the production of $ONOO^-$ in varying amounts), the predominating pool will differ depending on the oxidative state of BH4. Although much of this work was done in cardiovascular research, NOS is uncoupled in other inflammatory states such as diabetes [51, 52]. Our lab has shown that NOS is uncoupled in a variety of tumor types both *in vitro* and *in vivo*. We also showed that recoupling NOS with a precursor of BH4, sepiapterin (SP) leads to mitigation of colitis in mice [53]. Most recently, we showed that recoupling of NOS in breast carcinomas leads to tumor cell killing both *in vitro* and *in vivo* [42]. Therefore, even though tumor cells express NOS, due to the inflammatory oxidative microenvironment, NOS is uncoupled and producing ROS/RNS, which activate proliferative and anti-apoptotic pathways [54-58].

Implications of NOS Uncoupling and ROS/RNS Signaling

The coupling state of NOS determines whether NO or O_2^-/$ONOO^-$ molecules are produced. NO generally signals towards homeostatic, non-inflammatory pathways dependent and independent of PKG. For example, our lab and others have shown that PKG activation leads to an increase in p21 levels, leading to cell cycle inhibition [42-44]. ROS/RNS promote cancer cell survival through modulation of receptor tyrosine kinases

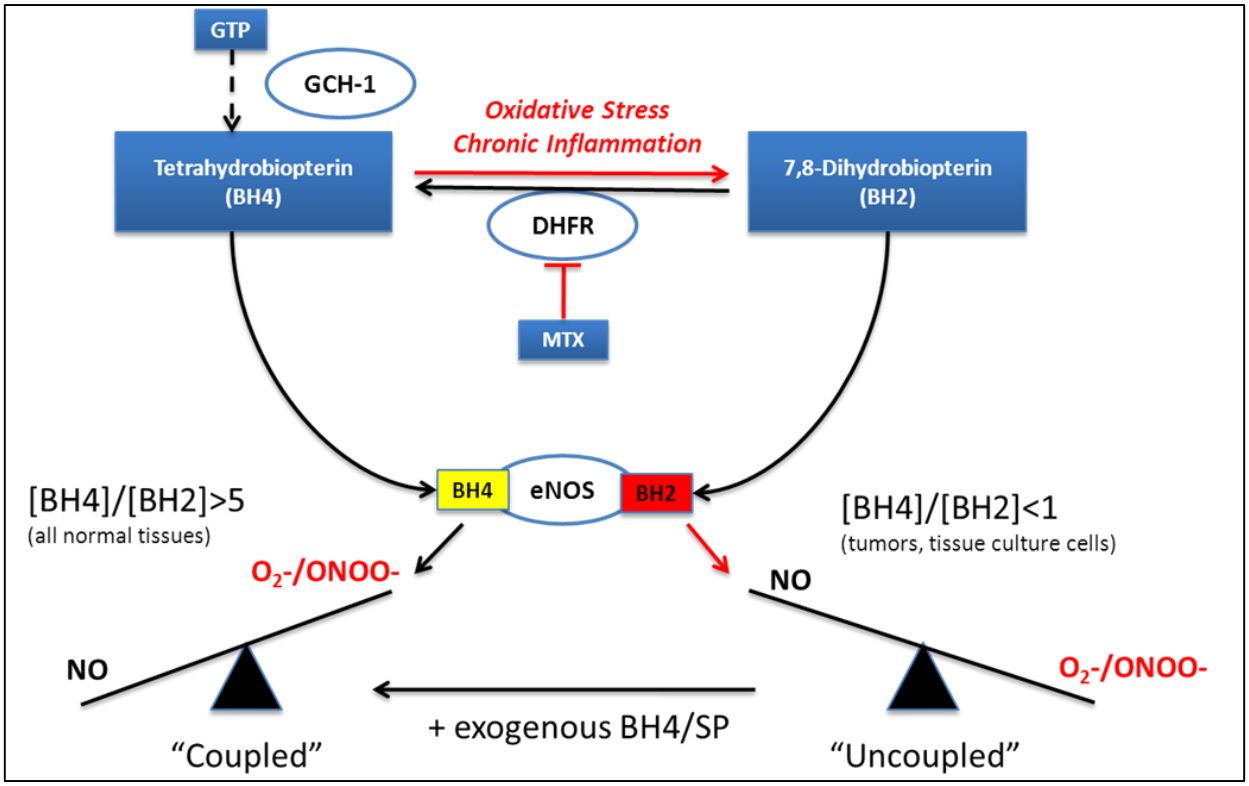

Figure 1.2: NOS Activity is Dependent on BH4:BH2 Ratio. In times of high BH4, NOS is coupled and predominantly produces NO, however in situations when BH2 is greater than BH4, NOS is uncoupled and produces superoxide and peroxinitrite radicals.

(RTK) [59]. RNS are generated by a reaction of ROS with NO. Peroxynitrite ($ONOO^-$), produced from the reaction of NO with O_2^-, is a powerful oxidizer which can react with amino acids, metal containing compounds, nucleic acids and plays a major role in cellular injury and cell death at high levels of $ONOO^-$. However at lower concentrations (such as during inflammatory states), $ONOO^-$ nitrates tyrosines on specific protein and leads to activation of cytoprotective mechanisms such as NFκB and Akt [56, 60-62].

Generation of ROS/RNS leads to altered cellular function through protein Tyr nitration and Cysteine (Cys) S-nitrosylation or S-oxidation. Tyrosine nitration involves the incorporation of a nitro group ($-NO_2$) to the ring structure of tyrosine residues resulting in the formation of 3-nitrotyrosine. Biologically relevant protein Tyr nitration has been proposed to occur through several mechanisms: the generation of NO_2 radicals, reaction of NO with tyrosyl radicals, and through generation of $ONOO^-$ [63]. Our work and others have validated the role of Tyr nitration and Cys S-nitrosylation as relevant cellular signaling mechanisms (Figure 1.3) [56, 61, 64-66]. Both processes are selective and reversible and these modifications can cause activation or inhibition of certain cellular pathways depending on the target. For example, our lab has demonstrated that nitration of IκBα is critical for the IR-induced activation of the pro-inflammatory transcription factor, NF-κB. Our lab has also shown that p53 can be nitrated and become activated due to low doses of NO donors or IR. Lastly, our lab has shown that physiological levels of NO/RNS lead to downregulation of BRCA1 leading to DNA damage repair via non-homologous end joining, rather than homologous end joining [67]. This may be a mechanistic explanation of how an increase in ROS/RNS can lead to an increase in genetic mutations.

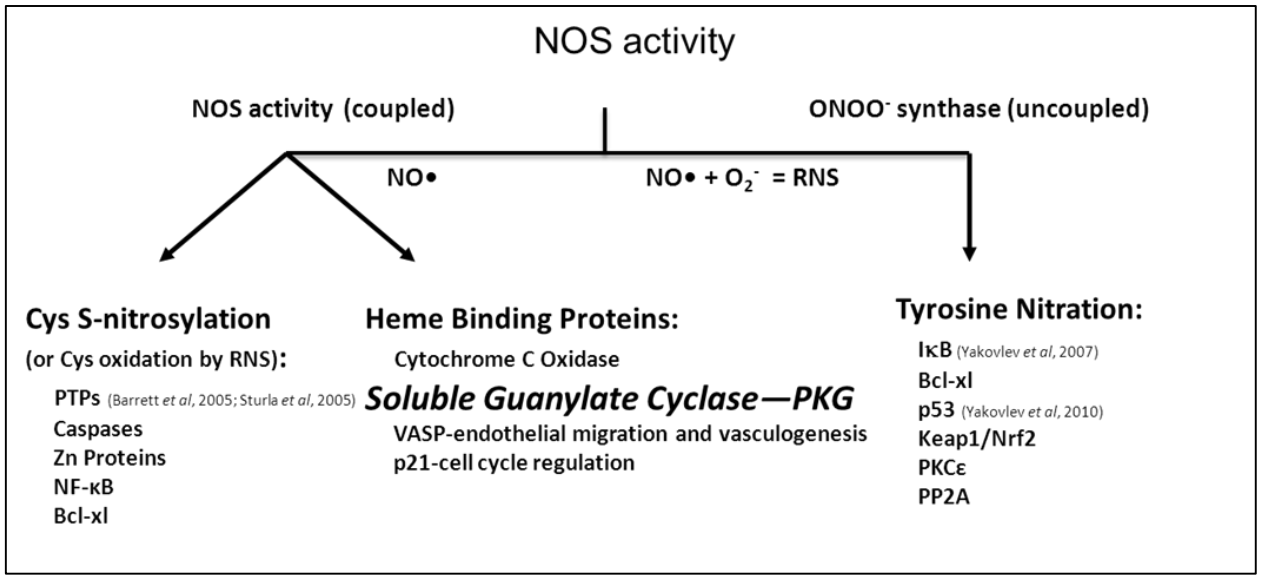

Figure 1.3: NOS Signaling is Dependent on Coupling State. Coupled NOS produces NO and signals towards anti-inflammatory/pro-apoptotic effector molecules such as PKG. However uncoupled NOS produces oxidative signaling, which leads to more proliferative and anti-apoptotic signals.

Akt, is an oncogenic protein that is activated in a variety of tumors. It is an integral component for activating pathways necessary for tumor growth, anti-apoptosis and metastasis. Recently, one mechanism of Akt regulation is via Cys S-nitrosylation. Cys. S-nitrosylation occurs through direct interaction of NO with the thiol group of cysteines resulting in the formation of a nitrosothiol (S-N=O) [68]. Numajiri et al showed that in areas of ischemia (with an increased amount of ROS/RNS and low NO) phosphatase with sequence homology to tensin (PTEN, phosphatase which inhibits PI-3K) was S-nitrosylated and inhibited, leading to the activation of Akt. However, in areas with higher NO, Akt was S- nitrosylated and inactivated [69]. The S-nitrosylation of Akt was shown to be at a specific cysteine, Cys-224 [68]. Thus a possible way tumor cells activate Akt is using uncoupled NOS (low levels of NO) to preferentially inhibit PTEN leading to increased Akt activity.

Many labs, including ours have shown that protein tyrosine phosphatases (PTPs) are also regulated by this S-nitrosylation mechanism. SHP-1 and SHP-2 have been demonstrated by our laboratory and by others to be regulated by S-NO [70-72]. The end result of this is to inhibit PTPs and activate receptor tyrosine kinases, such as Epidermal Growth Factor Receptor (EGFR) and Insulin Receptor, allowing for uncontrolled growth. S-nitrosylation of the active site cysteine of Caspases has been shown to inhibit apoptosis in many cell types such as hepatocytes, endothelial cells, and tumor cells [73-75]. The activation of proliferative and anti-apoptotic pathways is dependent on an inflammatory oxidative state which is produced due to the generation of ROS/RNS in the tumor cells and infiltrating immune cells. The end result is a deadly cycle of

inflammation and propagation of tumor cells leading to further inflammation and more malignant tumor cells.

Scope of Dissertation

The studies in this dissertation seek to determine what role NOS activity may have in progression of CRC and therapeutic potential of modulating the coupling state of tumor NOS. Earlier work in our lab showed that recoupling breast cancer cells with SP led to a decrease in β-catenin. I hypothesize that SP may have similar tumoricidal effects in colorectal cancer cells due to their dependency on Wnt signaling to promote tumorigenesis.

Our lab has shown that NOS is uncoupled in a variety of tumor cells both *in vitro* and *in vivo*. Using a precursor of BH4, sepiapterin (SP), we can recouple NOS and raise the BH4/BH2 ratio and lower superoxide production in tumor cells. SP feeds into the salvage pathway of biopterin metabolism and is converted via Sepiapterin Reductase (SR) and Dihydrofolate Reductase (DHFR) to BH4. We also showed that SP was tumoricidal in MDA-MB231 and MCF-7 cells, as well *in vivo* in xenografts of these cell lines as well as MMTV-Neu mice with spontaneous tumors. The recoupling of NOS led to activation of PKG and subsequent down regulation of β-catenin and activation of p21 (cell cycle inhibitor) as well as a decrease in Cyclin D1. The end result was decreased proliferation in tumor cells. We also examined the effects of sepiapterin in a murine model of CAC. Colitis and tumor formation are induced by the carcinogen Azoxymethane, and 3 one week cycles of dextran sodium sulfate (DSS) followed by normal drinking water. During the DSS cycles mice develop colitis which is apparent as weight loss, stool consistency and presence of blood in stool (collectively called Disease

Activity Index DAI). Mice develop tumors during the 10 week treatment course. SP was given prophylactically to a group of animals from the first DSS cycle and continued for 12 weeks. SP treated animals had a significantly less DAI as well as a diminished tumor burden.

In this thesis, I seek to determine the mechanism of decrease in β-catenin expression and to determine if SP can be used as a therapy (after tumors have developed) rather than prophylactically. Lastly, I will seek to determine mechanistic explanations of how tumor colorectal tumor cells maintain a decreased BH4:BH2 ratio. Studies in chapter 2 will show the effects of SP *in vitro.* The studies in chapter 3 will demonstrate that SP can be used therapeutically to have tumoricidal effects in murine CAC *in vivo* as well. Additionally, studies in chapter 3 will also seek to elucidate a mechanistic explanation for the decrease in BH4/BH2 ratio.

Chapter 2:

Recoupling of NOS *in vitro* decreases proliferation of colorectal tumor cells

BH4 is a necessary cofactor for the production of NO from NOS. Evidence has shown that NOS generates O_2^- under certain pathophysiological conditions. Both BH4 and its oxidized version, BH2 have equal affinity for NOS, thus their relative levels are important in regulating the balance of O_2^- and NO produced by NOS. In conditions where BH4 levels are low and high BH2, electron transfer in the active site of the enzyme becomes uncoupled from L-arginine oxidation resulting in the production of O_2^- instead of NO [47]. The uncoupled enzyme therefore becomes a generator of $ONOO^-$, which is produced rapidly by the reaction of O_2^- with NO produced in the same area. The reaction of NO with O_2^- is six times faster than the reaction of O_2^- with SOD so $ONOO^-$ formation is favored [60]. Figure 1.3 illustrates some of the cellular consequences of an uncoupled NOS. With uncoupling cell signaling shifts from sGC activation and S-nitrosylation towards reduced cGMP/PKG activity and $ONOO^-$ and protein nitration.

Earlier studies in our lab showed that in a variety of tumor cells and tumor tissues, BH4:BH2 ratios are lower than normal non-tumor tissue counterparts. As seen in Table 2.1 we measured BH4:BH2 ratios in a variety of *in vitro* cell lines. For example, in HT29 colon tumor cell line, we found its BH4:BH2 ratio was lower than normal colonic tissue. We next sought to determine if SP is able to raise BH4:BH2 ratios in both cells and animals. Exogenous SP was able to raise BH4:BH2 ratios both *in vitro* and *in vivo*. Another interesting finding of our study was that when we compared healthy colonic tissue with tumor colonic tissue from human patient samples, there was about a 2 fold

Normal Tissue	BH_4:BH_2 Ratio	*In vitro* Tumor Cell Lines	BH_4:BH_2 Ratio	BH_4:BH_2 +SP	*In Vivo*	BH_4:BH_2 Ratio	BH_4:BH_2 +1mg/kg /ml SP
Colon	7.1 ± 0.6	A431	0.3±0.5	2.06 ±0.6	Fadu	0.8±0.2	2.6±0.3
Lung	11.1 ±2.4	MCF-7	0.3±0.1	10.1±0.4	MCF-7	1.05±0.1	7.9±0.2
Liver	8.3±0.8	MDA231	1.0±0.1	5.8±0.2	MDA231	1.4±0.3	6.4±0.4
Kidney	13.4±1.2	SW1990	1.3±0.3	3.7±0.1	MMTV neu	1.2±0.5	3.9±0.2
Hu Paired Normal Colon	4.5 (3.5-6.1) p<.001 for paired student t-test	HT29	1.1±0.4	2.8±0.1	Hu Paired Colorectal Cancer	2.3 (1.5-3.5)	

Figure 1.4: Summary of BH4:BH2 Ratios in Different Tissues. BH4:BH2 Ratios were measured *in vitro* and *in vivo* tissues using HPLC. Ratios were measured in normal/non-tumor tissue, in untreated cultures as well as with SP treated cells and tumor bearing animals. Values are given ± SEM.

decrease in BH4:BH2 ratios in the tumors of these patients. Furthermore, we saw a decrease in O_2^- formation and decrease in nitro-tyrosine staining (a surrogate marker for ROS/RNS). Collectively, these results provide evidence that BH4:BH2 ratio is low in tumor tissue, NOS is uncoupled and ROS/RNS are elevated; however we can exogenously raise BH4:BH2 ratio by treating cells and animals with SP.

ROS/RNS at higher levels signal towards proliferative pathways. Our lab has shown that after IR and treatment with peroxynitrite, IκBα is nitrated which leads to active components of NF-κB, p65 and p50 translocation into the nucleus which lead to activation of multiple proliferative and inflammatory pathways. Many groups demonstrate that AKT is activated after oxidative stress as well as many other pro-survival and pro-inflammatory pathways [57]. The end result of this oxidative signaling is to help the cell survive an insult, or in the case of tumor cells to continue to grow, accumulate mutations and progress to metastatic state. By raising BH4:BH2 ratio, we can mitigate these pathways. We have shown decreased p65/p50, STAT3 and β-catenin in the nucleus after SP treatment in breast cancer cell lines. Most importantly, SP was able to decrease colony formation in breast cancer cell lines *in vitro* and *ex vivo*, thus the increase in BH4:BH2 is tumoricidal to breast cancer cell lines. In order to determine if SP has applications in multiple tumor types, we want determine if SP has similar tumoricidal effects in colorectal cancer cell lines. If, indeed it does, we also seek to determine the mechanism by which SP is acting in these colorectal cancer cell lines.

Materials and Methods:

A. Chemicals and Reagents

Pterin (#11.903), L-Sepiapterin (#11.225), Biopterin (#11.203), 7,8 Dihydro-L-Biopterin (#11.206) , and (6R)-5,6,7,8-Tetrahydro-L-biopterin dihydrochloride (#11.212) were from Schircks Laboratories (Jona, Switzerland). Sodium Deoxycholate (D6750), Sodium Thiosulfate (S7026), Silver Nitrate (S1179), Potassium Carbonate (209619), 40% Formaldehyde (F8775), Ascorbic Acid (A5960), Potassium Iodide (P-4286), Nω –Nitro-L-arginine (N5501), SB 216763 (S3442), S-Nitrosoglutathione (N4148) and Iodine (20,777-2) were from Sigma Aldrich. Hydrochloric Acid (A144-212), Sodium Hydroxide (SS255-1), HPLC grade Methanol (A452-4), HPLC grade Water (W5-4), DMSO (D128), HPLC grade Acetonitrile (26827-0040), Trifluoroacetic Acid and Perchloric Acid (A229) were purchased from Fisher Scientific. Peroxynitrite (81565), Nitrotyrosine Affinity Sorbent (389549) and cGMP EIA kit (581021) were purchased from Cayman Chemical. PBS (10010-023) RPMI 1640 (11875-093), Trypsin EDTA (15400-054), Penicillin Streptomycin (15240-062), Lipofectamine (50470) and Plus Reagent (10964-021) for transfection were purchased from Invitrogen. Matrigel (356234) was purchased from BD Biosciences and dihydroethidium (D11347) was from Molecular Probes. For animal studies involving treatment with SP, stock solutions of 0.8mg/ml in H_2O were frozen at -20˚C. When ready to use they were thawed and 1ml was diluted to 40ml in animal drinking H_2O. For tissue culture studies involving SP we used a 0.25% DMSO plus tissue culture medium as the solvent to make a 1mM stock solution which could then be diluted

as necessary (A .005% DMSO solution was used as vehicle/control treatment group). These solutions were made fresh each time cells were to be treated.

The following primary antibodies were used: Actin (sc-1616) were from Santa Cruz Biotechnology (Dallas, TX). anti-cyclin D1 (2978), anti-JNK1/SAPK (4668), anti-pGSK3β (9323) and anti-Stat3 (9131) were from Cell Signaling Technology (Danvers, MA). Anti-β-Catenin (610153) was from BD Transduction Laboratories (Franklin Lakes, NJ). The secondary antibodies used were conjugated with near infrared fluorophores designed for use with the Li-Cor Odyssey Infrared Imager: anti-rabbit 800 (611-132-003), and anti-goat 700 (605-730-002), were from Rockland Immunochemical (Gilbertsville, PA).

B. Cell Culture

HCT116 cells were purchased from ATCC (Manassas, VA) and HT29 and CACO2 were generously provided to us by Dr. Andrei Ivanov (VCU Department of Pharmacology and Toxicology). All cell lines were grown as monolayers in McCoys 5A Media (Life Technologies) supplemented with 10% FBS and 50units/ml penicillin and streptomycin. Cells were incubated at 37˚C in 5% CO_2. Cells were passaged as necessary.

C. BH4 and BH2 measurements

HCT116 and HT29 cells were plated at a density of $2x10^6$ cells/100mm dish and were allowed to adhere overnight. The next day cells would receive the indicated treatment and would then be placed back in the incubator for the duration of treatment. When the cells were ready to be harvested the dishes were washed in ice cold 1x PBS three times. After the final wash all PBS was

aspirated off and the cells were then lysed in 1ml of ice cold 0.1N HCl and placed in a 1.5ml microcentrifuge tube. The samples would sit on ice for 20min and then] centrifuged for 20min at 13,200 RPM. The supernatants were divided into aliquots and placed either into a -80°C freezer or analyzed immediately for BH4 and BH2 content. The pellets were dissolved in Laemmili sample buffer for protein analysis by Western blot. To analyze biopterin levels in tumors or other mouse tissues animals were anesthesized with isofluorane and euthanized by cervical dislocation. Once the animal was sacrificed we harvested the desired tissue and snap froze it in liquid nitrogen. The tissue was either placed in the -80°C freezer or immediately homogenized in 10 volumes of 0.1N HCl with a pestle and mortar kept on ice. The resulting tissue homogenate was centrifuged for 20min at 13,200 rpm and the supernatant was be stored in aliquots at -80°C.

The protocol for HPLC analysis was adapted from Woolfe et al (1983). Three solutions were needed in order to perform the acid/alkaline oxidation: 2%I_2/3%KI in 0.1N HCl, 2%I_2/3%KI in 0.2N NaOH, and 2.5% Ascorbate in 0.4N perchloric acid. 100µl of sample was incubated with 62.5µl of the HCl solution in one tube while another 100µl of sample was incubated with the NaOH solution for 1h at room temperature in the dark. After 1h, 0.5 vol of the ascorbate solution was added to each tube and the samples centrifuged at 12,000 RPM for 10min. 50µl of the resulting supernatant from each sample was separated by HPLC on a Whatman RTF partisphere column using 5% methanol as the mobile phase at a flow rate of 1.0ml/min and fluorescent detection at 350/450nm. To determine the

BH4:BH2 ratio I compared the acidic and alkaline chromatograms for each sample. Under acidic conditions both BH4 and BH2 were converted to biopterin and eluted in one peak, while under alkaline conditions BH4 was converted to pterin and now eluted in a different peak. Comparing the areas under the curve I was then able to obtain the BH4:BH2 ratio.

D. Cell Viability Assays (WST)

WST-1: Cells were washed, trypsinized and counted in a hemocytometer. This assay is performed in a 12 well plate and samples are plated in triplicate. 50 $x10^3$ cells/well in 2mL of medium were plated and allowed to incubate overnight to adhere. To determine cell viability 4µl of WST-1 reagent was added to the well and allowed to incubate for 3 hours before. The formazan that is formed by metabolically active cells is then quantified by spectrophotometer at 420-480nm. For our experiments involving SP treated cells, if the treatment was longer than 24 hours, fresh media with appropriate concentration of SP was put on the cells every day until the end of the treatment period. Appropriate concentrations of SP plus Media was used as the blank during plate reading.

E. Clonogenic Assay:

Cells were trypsinized and plated in 10cm dishes. 200 cells were plated in the control dishes while 500 cells were plated in the treatment groups. Dishes were treated with varying concentrations of SP 16 hours after plating. When the colony size reached 50 cells, cells were fixed in -20˚C methanol, stained with 0.5% crystal violet and counted.

F. Western Blot Analysis

Protein was extracted from ~80% confluent cell layer in (150uL/6cm dish) in RIPA lysis buffer (50 mM Hepes pH 7.4, 150 mM NaCl, 1% Triton X-100, 1% sodium deoxycholate, 0.1% SDS, 5 mM EDTA) and processed under reducing conditions. Alternatively tissue culture cells were harvested in 1X Laemmli sample buffer. Proteins were resolved by SDS-polyacrylamide gel electrophoresis and transferred to nitro-cellulose membranes. Membranes were incubated with the primary antibody of interest overnight at 4°C. Blots were developed using IR 700 or IR 800 conjugated secondary antibodies (Rockland Immunochemicals, Gilbertsville, PA) diluted 1:10,000 and imaged/analyzed using the Odyssey Licor system.

G. shRNA Lentiviral Transduction

GSK3β shRNA Lentiviral Particles-A (sc-270460-V) and Control shRNA Lentiviral Particles-A (sc-10808) were purchased from Santa Cruz Biotechnology (Dallas, TX). In a 12 well plate, HCT-116 cells were plated to achieve ~50% confluence the following (infection) day in complete McCoy's Media (10% FBS). 1mL/well of complete media with 5ug/mL of Polybrene (sc-134220) and 20uL of appropriate Lentiviral Particle was prepared as infection media. Complete growth media was replaced with infection media and incubated overnight for 12 hours. Media was changed to fresh complete growth media and incubated overnight. To select stable clones, cells were split 1:3 from original 12-well plates and grown for 48 hours in 10cm dishes. shRNA expressing clones were selected by treating dishes with 10ug/mL of Puromycin dihydrochloride (sc-108071) in complete growth media. Fresh puromycin was replaced every 3-4 days. After 2 weeks of growth under puromycin selection, cells were split 1:50 into multiple dishes.

Single colonies were picked under sterile conditions and grown to confluence under puromycin selection. These clones were then analyzed via western blot analysis for GSK3β expression.

H. TCF/LET Luciferase Reporter Assay

HCT-116 cells were plated at a density of $1x10^5$ cells/60mm dish and were allowed to incubate for 24 hours to adhere. Since cells were to be transfected with the TCF/LEF construct 24 hours before harvesting, I had to treat cells with SP accordingly. All cells were placed in fresh 10% medium after transfection. The cells were washed in ice cold PBS and harvested in the lysis buffer provided in the kit. I followed the protocol in the kit exactly

I. **AKT Activity Assay**

The Akt activity assay kit was purchased from Cell Signaling Technology (#9840) and their protocol followed. Briefly, cells were lysed in provided buffer and Akt was immunoprecipitated overnight using AKT Ser473 antibody-immobilized beads. After washing the beads (3X), the kinase assay was performed with GSK3β substrate and 10mM ATP at 30ºC. After termination, the samples are analyzed via western blot, blotting for phosphorylated GSK3β. Western blots were quantified by densitometry and the average for 3 experiments was normalized to control.

J. Biotin Switch Assay: Analysis of S-nitrosylated Proteins

This method was used to determine Cys S-nitrosylation. For total cellular S-nitrosylation, cells were grown to 80% confluent and then harvested. For analysis of a specific protein it was typically overexpressed. HCT-116 cells,

$1.2x10^6$ cells were plated and allowed to adhere overnight. The resulting cell lysate was centrifuged for 5 min and the supernatant was mixed with blocking buffer (250mM Hepes pH 7.7, 1mM EDTA, 0.1mM neocuproine, 2.5% SDS, 20mM MMTS) to block all free sulfhydryls. The sample was then mixed with acetone to precipitate the proteins to remove MMTS. The preceding steps are done under conditions of low light as to not create additional reactive Cys from exposure to UV. The pellet is resuspended in Hens buffer (25mM Hepes 7.7, 0.1 mM EDTA, 10µM neocuproine, 1% SDS) to which is added biotin-HPDP and ascorbate to a final concentration of 1mM. Samples incubate for 1 hour at room temperature. Proteins are again precipitated with acetone to remove excess biotin. Proteins are resuspended in neutralization buffer (20mM Hepes, 100 mM NaCl, 1mM EDTA, 0.5% Triton X-100) and the biotin labeled proteins are purified on streptavidin-agarose beads overnight, washed the following day with wash buffer (neutralization buffer with 600mM NaCl) and then eluted in sample buffer containing β-mercaptoethanol. The samples were then resolved by SDS-Page. Western blots are probed with streptavidin for total s-nitrosylation or with antibodies for specific proteins.

Results:

Sepiapterin Raises BH4:BH2 ratio in colorectal cancer cells and decreases proliferation

Previous studies in the lab had shown that many tumor cell lines have decreased BH4:BH2 ratios compared with their normal tissue counterparts. In order to determine if SP is having any effects on our colorectal cell lines, we first needed to determine if SP was able to raise BH4:BH2 ratios significantly in CRC cell lines. HCT-116 and HT29 cells were treated with 20μM SP for 24 hours and analyzed for BH4:BH2 ratio via HPLC (Table 2.2). SP treatment increased the BH4:BH2 ratio by more than two fold in HT29 cells and about a 5 fold increase in the ratio in HCT-116 cells compared to baseline. Next the effects on proliferation of HCT-116 cells when treated with SP were determined via WST assay. Treatment by SP of HCT-116 was able to decrease cell growth, as measured by WST absorbance during a 5 day treatment course (Figure 2.1). Colony formation assays were used to determine if SP has direct cell killing effects. Increasing concentrations of SP led to increased cell death. A 30-40% cell killing effect at 20μM in both HCT-116 and HT29 cell lines was seen, which is the concentration used in further experiments (Figure 2.2). These data suggested that SP did have a cytotoxic effect on CRC cell lines and next we sought to determine the mechanism of action of SP.

Table 2.2: BH4:BH2 Ratios in Colorectal Cancer cells

	BH4:BH2 Ratio	BH4:BH2 + SP 20μM
HT29	1.1 ± 0.4	2.8 ± 0.1
HCT116	2.3 ± 0.2	11.6 ± 2.3

BH4:BH2 Ratios were measured *in vitro* colorectal cancer cell lines using HPLC. Ratios were measured in untreated cultures as well as with SP treated cells. In both types of cell lines, SP was able to raise BH4:BH2 ratio. Values are given ± STD.

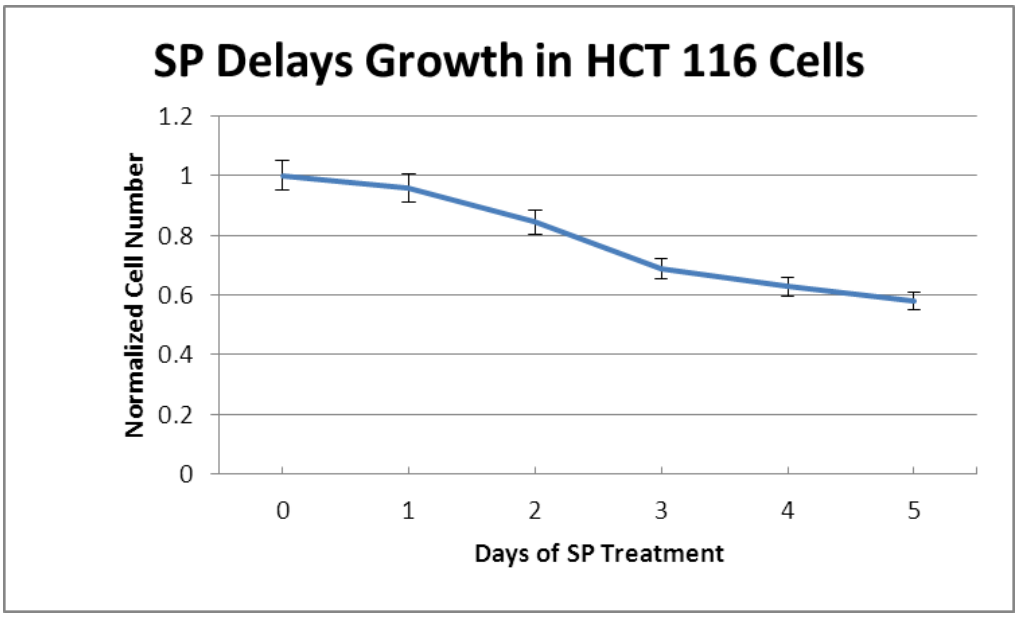

Figure 2.1 WST Cell Proliferation Assay. HCT-116 Cells were treated with SP for noted number of days and after treatment with WST, absorbance was measured to estimate cell proliferation. SP was able to decrease cell proliferation after 3 days of treatment. Absorbance was normalized to untreated cells.

A.

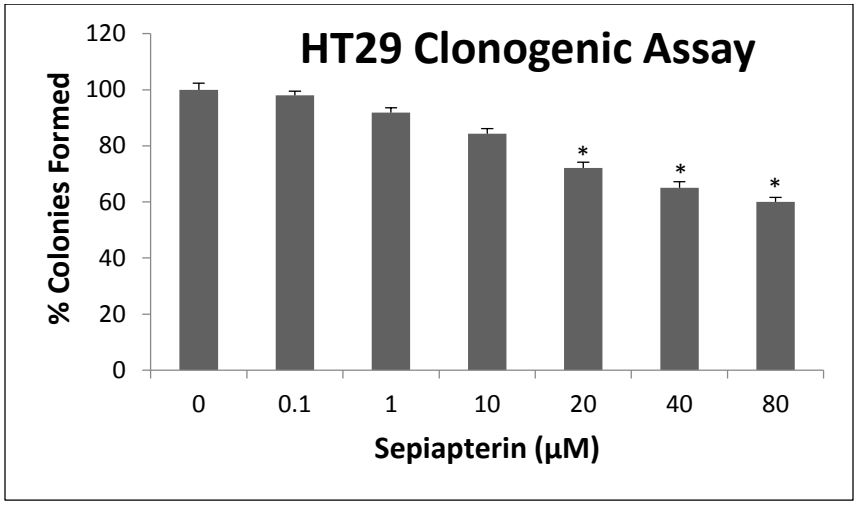

B.

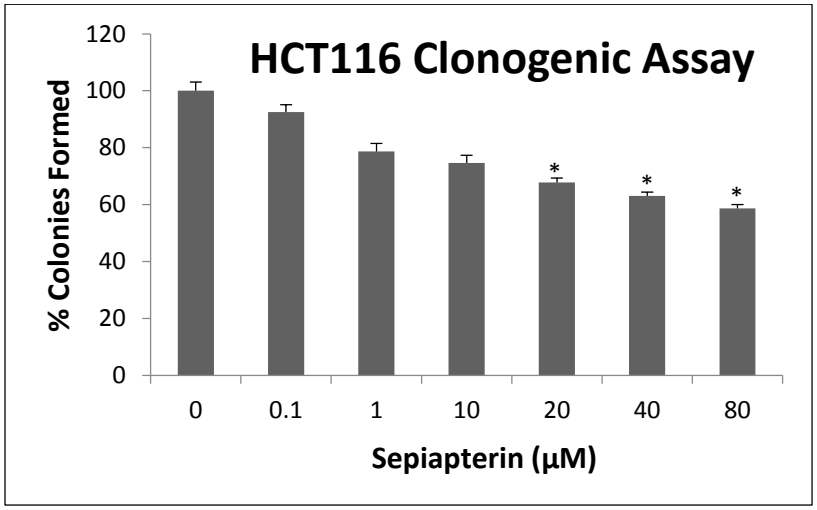

Figure 2.2 *In Vitro* Clonogenic Assays. (A)HCT-116 Cells and (B) HT29 Cells were treated with SP at the concentrations noted for 24 hours. Cells were then plated in triplicate at counts of 100, 500 and 1000 cells/dish and allowed to grow to visible colonies. Colonies were normalized to untreated cells and assessed for statistical significance using the student's t-test. *p <0.05 as compared to untreated cells.

Sepiapterin decreases expression of β-catenin by activating GSK-3β in colorectal cancer cell lines

Earlier studies in the lab demonstrated that β-catenin levels were downregulated in breast carcinoma lines. HCT-116, HT29 and CaCo2 CRC cell lines were used to determine if SP had any effect on β-catenin expression. In all three cells lines we tested, β-catenin levels were decreased after 4 and 5 day treatment course (Figure 2.3). To confirm that SP was able to decrease transcription activity of β-catenin a LET/TCF luciferase promoter activity assay was employed. In HCT-116 cells, SP was able to significantly decrease LET/TCF driven luciferase expression after 3 and 5 days of treatment (Figure 2.4). The next question to answer was to determine what was causing decreased β-catenin levels. AKT is potent activator of Wnt signaling. AKT phosphorylates GSK3β at Serine 9 causing it to become inactive. GSK3β is then unable to phosphorylate β-catenin, leaving β-catenin able to translocate to the nucleus and bind its target DNA. AKT is also activated during times of oxidative stress. Since SP increases BH4:BH2 ratio thereby decreasing oxidative stress, AKT activation should also be decreased. Phosphorylation of Ser473 on AKT (marker for its activation) was measured via western blot and in our colorectal cell lines there was decreased phosphorylation of Ser473 (Figure 2.5). Next, an *in vitro* kinase activity assay was used to determine if indeed AKT activity was decreased after SP treatment. As seen in Figure 2.6A, AKT activity was significantly decreased after SP treatment. GSNO (an NO donor) was used as a positive control because we suspected AKT was S-nitrosylated due to the increase in NO formation from NOS. Previous work in other labs has shown that NO donors can S-nitrosylate AKT rendering it inactive. Using the biotin switch method, SP was able to S-nitrosylate AKT and in conjunction with the western blot and activity

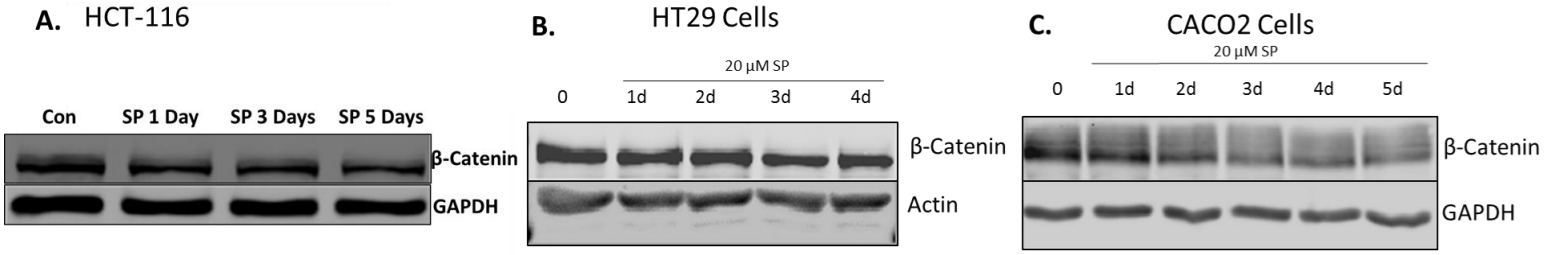

Figure 2.3 Western Blot Analysis of β-catenin after SP Treatment. (A)HCT-116,(B) HT29 and (C) CaCo2 cells were treated with SP at 20 μM for 1-5 days. Cells were then lysed and analyzed via western blots for protein analysis. Representative blots are shown from experiments done at least 3 times in each cell line.

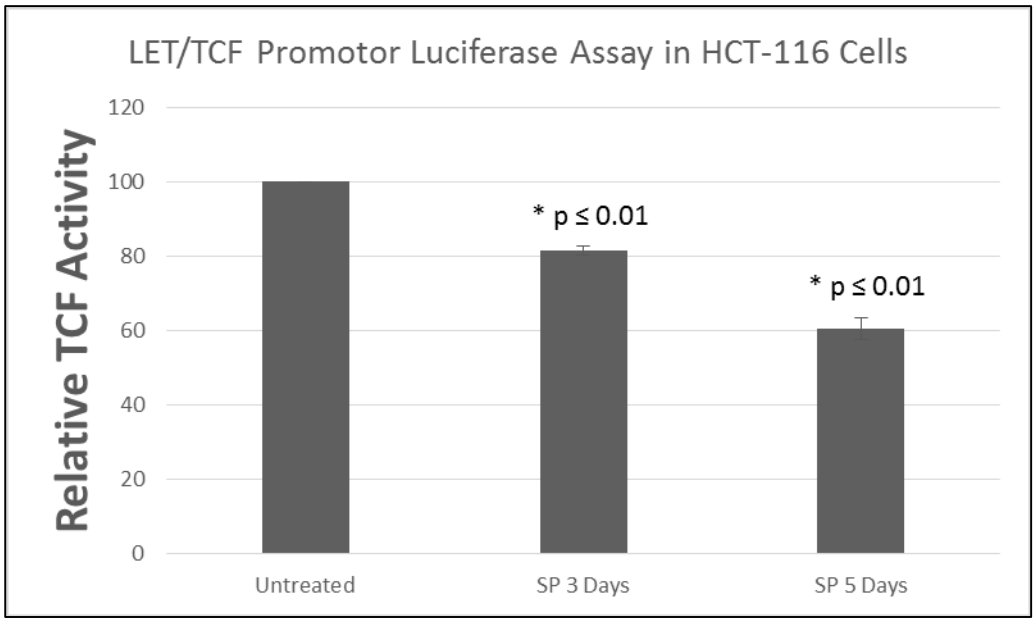

Figure 2.4 LET/TCF Luciferase Promotor Activity Assay. HCT-116 cells were treated with 20µM SP for 3 and 5 days continuously. 24 hours before harvesting cells were transfected with a plasmid encoding luciferase driven by nuclear β-catenin binding to LET/TCF promoter site. Luciferase activity was measured 3 and 5 days post SP treatment. Results are quantified from 2 separate experiments done in triplicate. Results are normalized to untreated cells and reported as ± SEM. Student's t-test was used to assess for statistical significance.

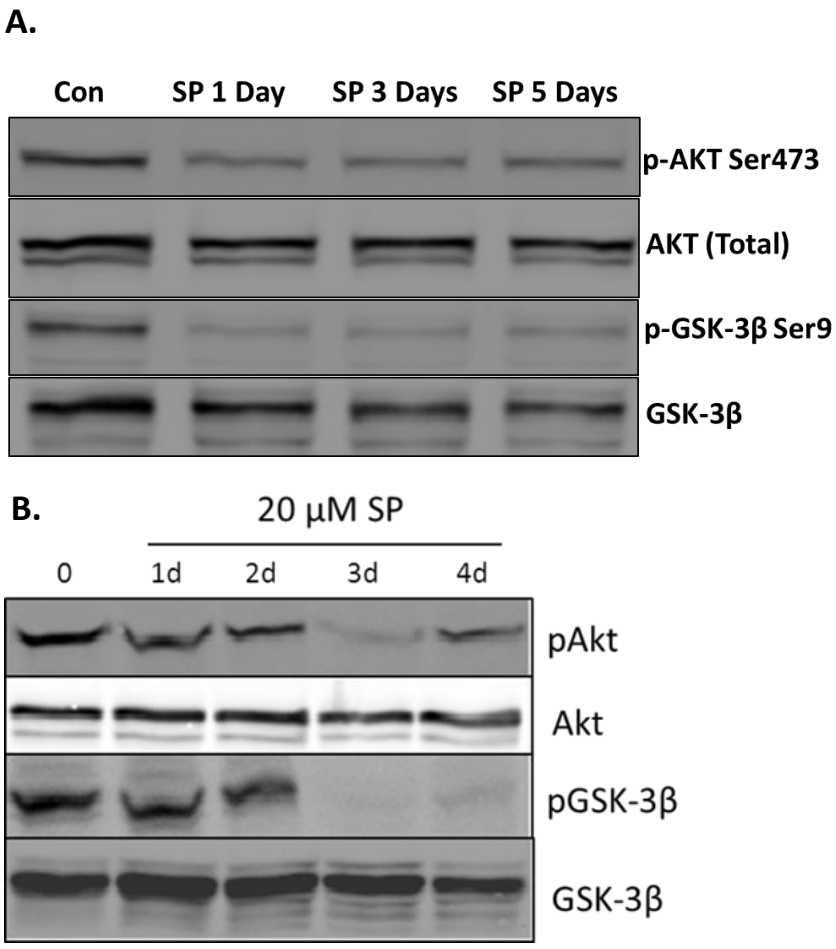

Figure 2.5 Western Blot Analysis of AKT and GSK3β after SP Treatment. (A)HCT-116, (B) HT29 cells were treated with SP at 20 μM for 1-5 days. Cells were then lysed and analyzed via western blots for protein analysis. Representative blots are shown from experiments done at least 3 times in each cell line.

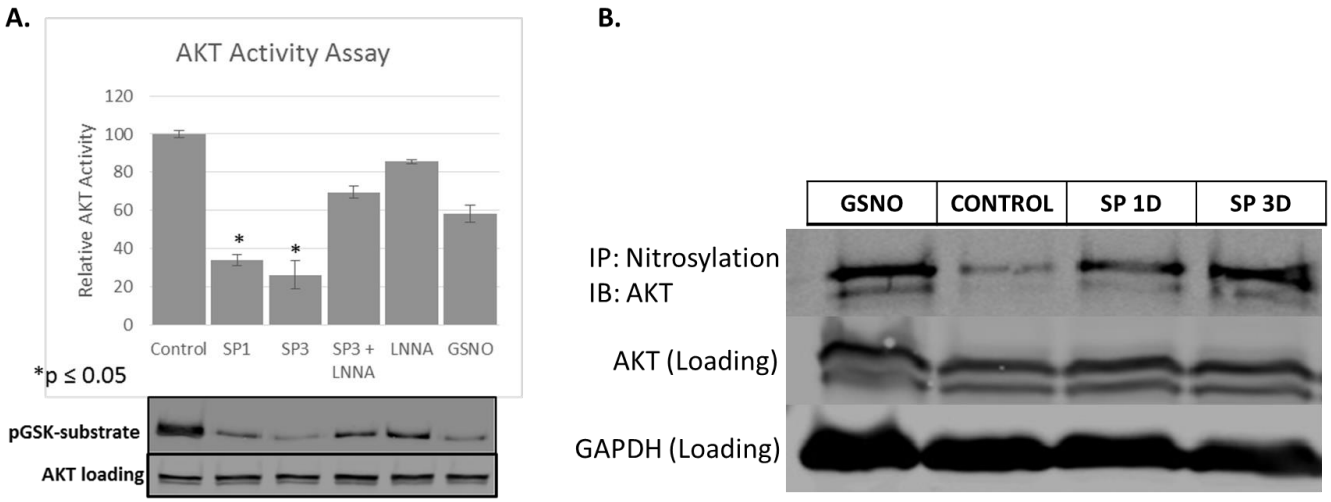

Figure 2.6 AKT Activity Assay and S-Nitrosylation after SP Treatment. (A) AKT activity assay, HCT-116 were treated with 20µM SP and/or 100nM L-N^G-Nitroarginine (L-NNA, NOS inhibitor) for specified days and 1mM GSNO (added directly to cell lysate, as positive control). AKT in vitro kinase activity was measured, bar graph is average of activity measured in 3 assays performed with a representative blot from one experiment.*p< 0.05, using student's T-test. (B) Biotin Switch Assay in HCT-116 cells with 20µM SP treatment after 1 or 3 days and GSNO (as positive control), representative blot from 2 separate and independent experiments is shown.

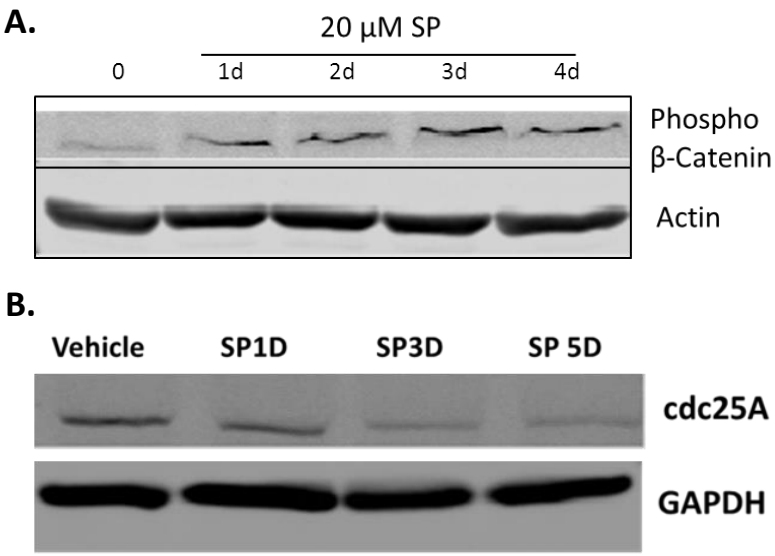

Figure 2.7 Western Blot Analysis of downstream targets of GSK3β after SP Treatment. (A)HCT-116 cells were treated with 20µM SP for specified days and analyzed for phosphorylation of β-catenin at Ser 33/37 (A) and cdc25A (B) which is another target of GSK3-β regulation. Representative blots are shown from experiments done at least 3 times in HCT-116 cells.

assays, cause it to lose its activity (Figure 2.6B). Due to the decrease in AKT activity, we expected to see less Ser9 phosphorylation of GSK3β, which was the case in both HT29 and HCT-116 cells (Figure 2.5). Lastly, we saw increased phosphorylation of β-catenin at Ser33/37 (GSK3β's phosphorylation site) which marks β-catenin for degradation in HCT116 cells (Figure 2.7A). To confirm increased GSK3β activity, we saw decreased levels of CDC25A, an important activator of the cell cycle which is also phosphorylated by GSK3β and subsequently degraded (Figure 2.7B). Thus, in CRC cells, SP leads to decreased activation of AKT and corresponding increased activation of GSK3β, causing decreased β-catenin and CDC25A levels leading to decreased proliferation and cell death. This mechanism seems to be dependent on GSK3β.

Pharmacological inhibition of GSK3β or genetic knockdown leads to an abrogation of SP's effects.

GSK3β in colorectal cancer cells is integral in regulating Wnt signaling and a variety of anti-proliferative and apoptotic pathways. Furthermore, our previous work shows SP is activating GSK3β to downregulate β-catenin levels in HCT-116 and other colorectal cancer cell lines. Thus to confirm GSK3β's role in SP's anti-proliferative effects in these cells, we decided to treat HCT-116 cells with SB 216763 (Sigma), a specific inhibitor of GSK3β. Treatment with SB 216763 and SP blocked the loss of β-catenin when cells were concurrently treated with SP (Figure 2.8). To confirm the effects of pharmacologic inhibition of GSK3β, we decided to clone stably transfected cells expressing shRNA for GSK3β knockdown. Genetic knockdown is confirmed in Figure 2.9. We next performed experiments to determine effects of SP in scramble and GSK3β knockdown cells. Our results show that with genetic knockdown of GSK3β, we lose the effects of SP on β-catenin. Using shGSK3β cells we also examined the effect

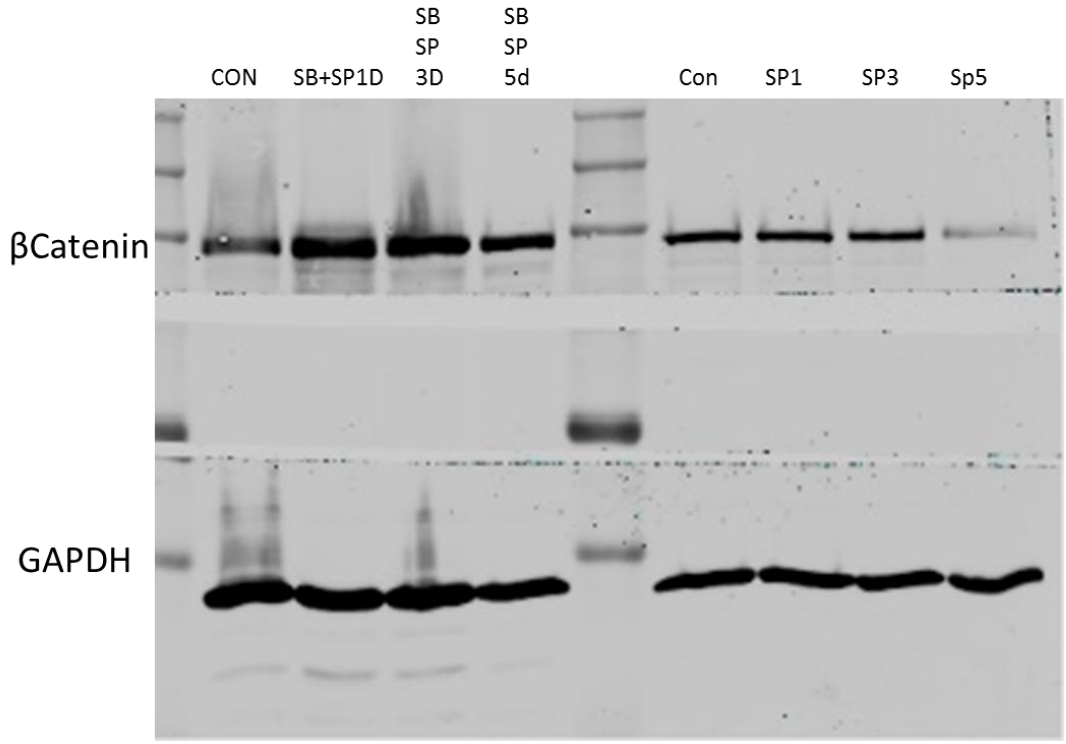

Figure 2.8 Western Blot Analysis of SP effects with GSK3β Pharmacologic Inhibition. HCT-116 cells were treated with 20μM SP and/or 10μM of SB216763 (SB) for specified days and analyzed for β-catenin expression. CON = untreated cells. Representative blots are shown from experiments done 3 times in HCT-116 cells.

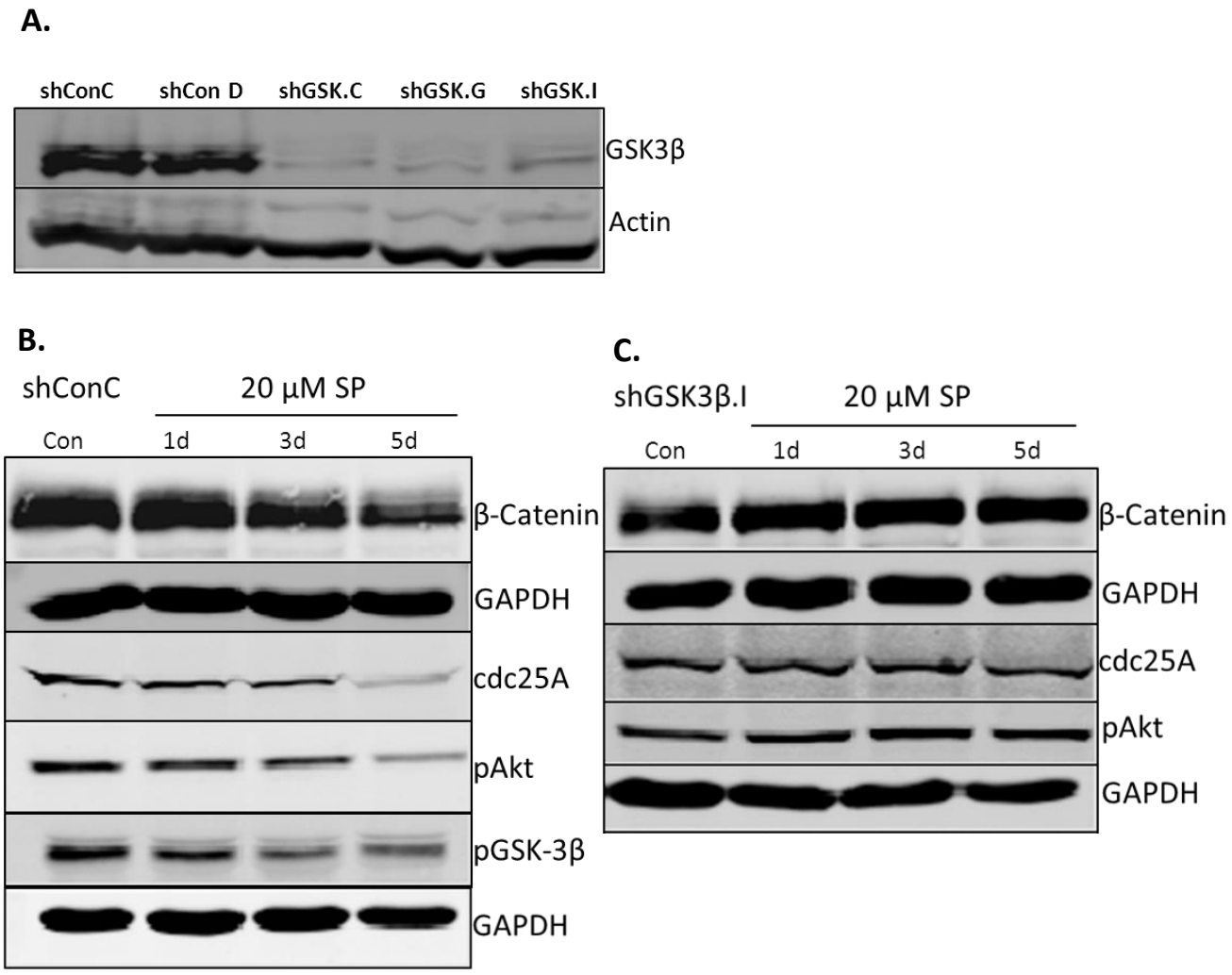

Figure 2.9 Western Blot Analysis GSK3β Knockdown in HCT-116 Cells after SP Treatment. (A) HCT-116 cells were transfected with lentivirus containing shGSK3β or scramble shRNA. Single colonies were picked, passaged and analyzed for GSK3β expression. 3 different clones for GSK3β knockdown and 2 clones for shSCR were used in subsequent studies. (B) shCONC or (C) shGSK3β.I were treated with 20µM SP for specified days and analyzed for SP's effects after GSK3β knockdown. Representative blots are shown from experiments done at least 3

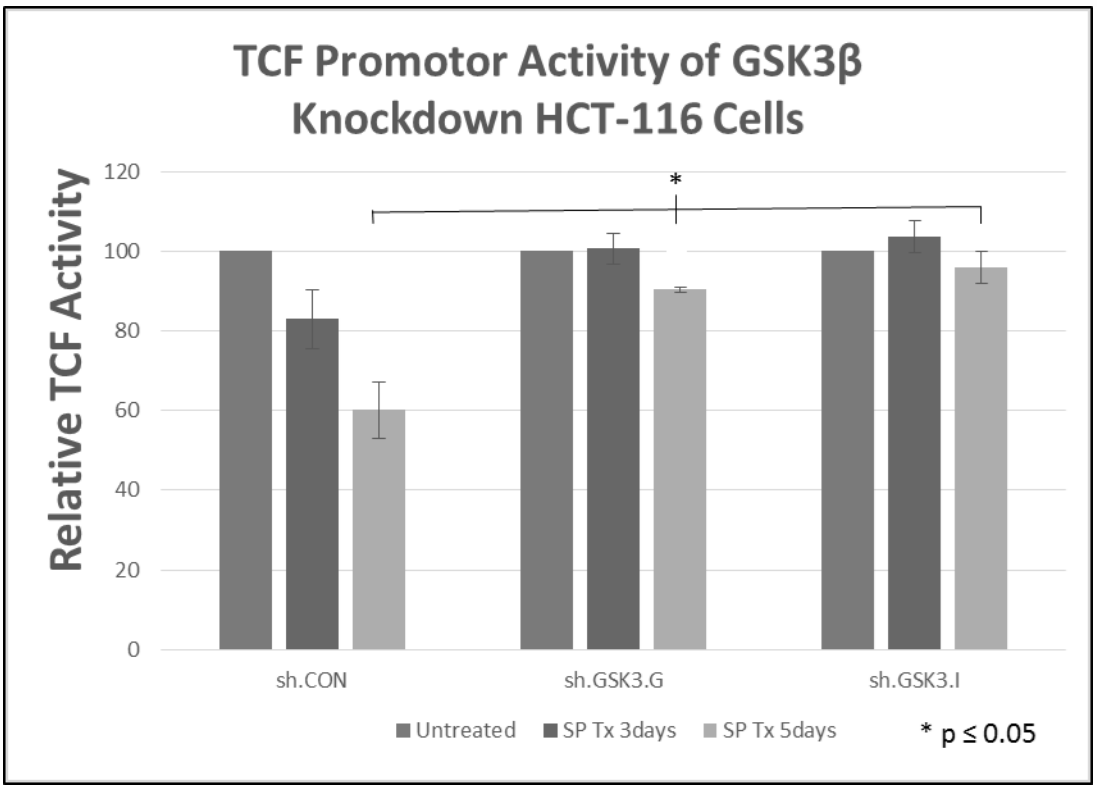

Figure 2.10 LET/TCF Luciferase Promotor Activity Assay with GSK3β Knockdown HCT-116 Cells. HCT-116 cells transfected with GSK3β or scramble shRNA were treated with 20µM SP for 3 and 5 days continuously. 24 hours before harvesting cells were transfected with a plasmid encoding luciferase driven by nuclear β-catenin binding to LET/TCF promoter site. Luciferase activity was measured 3 and 5 days post SP treatment. Results are normalized to untreated cells and reported as ± SEM. Student's t-test was used to assess for statistical significance between untreated shCON 5D, versus shGSK3.G and shGSK3.I at 5 days. *$p \leq 0.05$

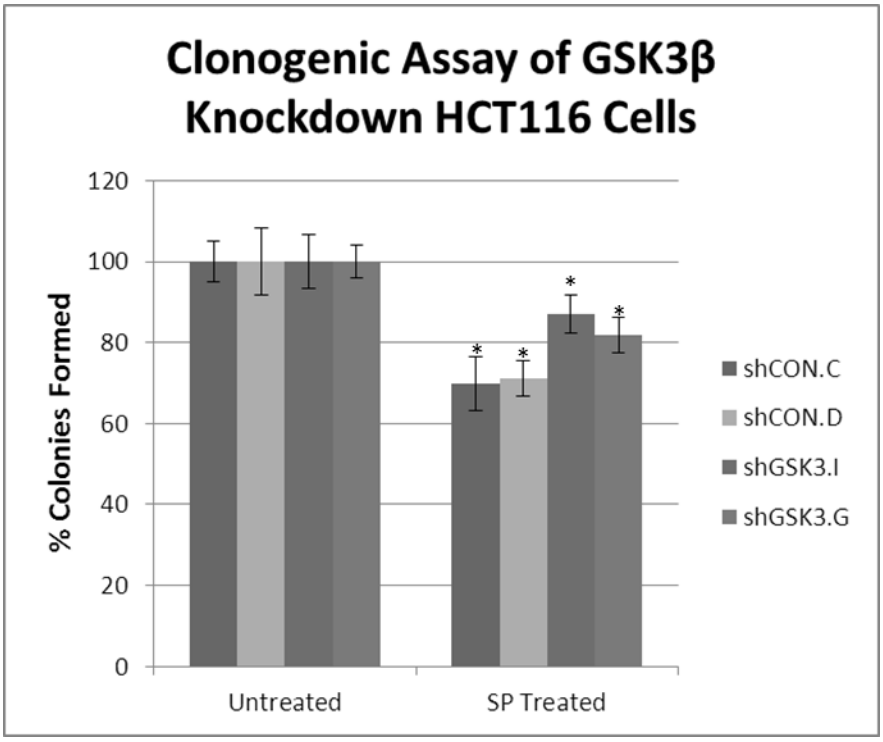

Figure 2.11 *In Vitro* Clonogenic Assays with GSK3β Knockdown HCT-116 Cells. HCT-116 cells transfected with GSK3β or scramble shRNA were treated with 20 µM SP for 24 hours. Cells were then plated in triplicate at counts of 100, 500 and 1000 cells/dish and allowed to grow to visible colonies. Colonies were normalized to untreated cells and assessed for statistical significance using the student's t-test between shCON.C and shCON.D and shGSK3.I and shGSK3.G after SP treatment *p <0.05.

of SP on LET/TCF luciferase activation (Figure 2.10) as well as colony formation in GSK3β knockdown HCT-116 cells (Figure 2.11). In both cases, knockdown of GSK3β caused mitigation of SP's effect on colony formation as well as abrogated the loss luciferase expression in our assay. However, we did not see a complete loss of SP's effect on colony formation in these cells, suggesting SP has other mechanism(s) which can decrease cell proliferation.

Discussion:

The objective of the experiments in this chapter were to determine what effects SP had on colorectal tumor cells. To this end, the studies showed that SP was able to increase the BH4:BH2 ratio in CRC cells. SP also led to a decrease in cell proliferation of HCT-116 cells, as well as decrease the colony formation ability in HCT-116 and HT29 cells. Next we sought to determine the mechanism of action of SP in these cell lines. SP decreased the protein levels of β-catenin, and as a consequence----- (via luciferase activity assay) in HCT-116 cells. We also examined regulators of Wnt signaling, namely Akt and GSK3β. Akt negatively regulates GSK3β and leads to accumulation of β-catenin. When we treated our CRC cells with SP, we saw less activation of Akt and increased GSK3β activation. GSK3β led to phosphorylation of β-catenin and its downregulation. SP also led to the S-nitrosylation of Akt, a modification dependent on an increase in NO. Inhibition and genetic knockdown of GSK3β led to abrogation of SP's effects of β-catenin levels, LET/TCF activation as well as a mitigation of cell death.

Previous work in our lab had shown that SP's effects in breast cancer cells were mainly through activation of Protein Kinase G. Although our colorectal cells express PKG, none of the targets of PKG showed any changes, such as p21, p27 and cyclin D.

A possible explanation for why I did not see PKG activation in CRC cells was due to the high levels of cGMP phosphodiesterases (PDEs) in colorectal tumors [76-78]. Thus even though we elevated NO levels, cGMP levels would not rise due to PDE activity. Future studies can combine SP with PDE inhibitors to increase SP's tumoricidal effects. Although these studies focused on AKT and GSK3β, we cannot rule out other anti-proliferative/pro-apoptotic pathways as well, due to the observation that there was cell death in HCT-116 cells even with GSK3β knockdown (Figure 2.11). In fact, we have seen in our CRC cells, decrease of STAT3 Tyr705 phosphorylation after SP treatment. Current studies are underway to examine SP's effects on STAT3. Earlier work in our lab has shown that STAT3 activation, as well as NFκB, is decreased with SP treatment as well. We believe that by increasing the BH4:BH2 ratio and re-coupling NOS, SP decreases the oxidative stress in cancer cells. Tumor cells rely on an oxidative environment to activate proliferative pathways which help incur mutations, provide a selective growth advantage and eventually lead to more invasiveness and metastasis.

S-nitrosylation of AKT has been shown to be an important regulator of AKT activity [69]. Numajiri et al showed that in areas of low NO, PTEN is preferentially S-nitrosylation leading to an increase in AKT activity, however when the NO concentration is high, AKT is S-nitrosylated at Cys-224 and inhibited. This mechanism may be an important sensor for oxidative stress and fits with NOS uncoupling during ischemia and inflammation. During ischemia, in order to survive, cells must activate pro-proliferative mechanisms such as AKT-dependent pathways. A common denominator in inflammatory states such as ischemia (and the tumor microenvironment) is a decrease in BH4:BH2 ratio. The drop in BH4, leads to an uncoupled NOS and a decrease in the

relative NO concentration. This leads to an inhibition of PTEN, activation of AKT and downstream signaling leading to proliferation and survival. Tumor cells may use this mechanism to activate AKT to continue proliferation and avoid apoptosis. By treating cells with SP, we are able to recouple NOS and increase NO production and inhibit AKT activity. A future experiment to corroborate this finding will be to see what happens to levels PTEN S-nitrosylation with SP treatment. We would suspect less S-nitrosylation, although it is unclear how the concentration difference effects which protein is S-nitrosylated. Perhaps PTEN has a more readily accessible cysteine as compared to AKT. Another possible explanation could be the subcellular location of NOS relative to the location of AKT and PTEN, thus affecting the relative amount S-nitrosylated proteins. Lastly, our lab and others have realized a potential limitation of the biotin switch assay. This method detects all oxidized cysteines, not just S-nitrosylated (which is NO mediated) but also sulfenic and sulfonic acid oxidized cysteine modifications which are irreversible $ONOO^-$ /O_2^- dependent [79, 80]. Thus in the ischemic state, which is rich in ROS/RNS, PTEN may actually be modified to an oxidized cysteine, whereas in states where NO concentration is higher (with lower ROS/RNS levels) AKT is preferentially S-nitrosylated. The end result will still be similar, PTEN will be inhibited due to its oxidized cysteine in ischemic state, allowing AKT activation. In our biotin switch assays, we used ascorbate which leads to selective immunoprecipitation of s-nitrosylated proteins and avoids sulfonic/sulfenic acid derivatives.

As mentioned earlier in the introduction, there are two different schools of thought on NOS and NO signaling in cancer cells. Many groups have shown, including our lab, that inhibition of NOS leads to decreased tumor growth and proliferation [42,

81-85]. These studies have also shown that NO donors can decrease tumor proliferation and increase apoptosis. Other groups have shown that NOS and treating cells with NO donors leads to tumor growth [38, 45, 86-90] . We believe one of the main reasons for these conflicting reports is the coupling state of NOS. We have shown that in a variety of tumor cell lines both *in vitro* and *in vivo*, NOS is uncoupled. An uncoupled NOS produces ROS/RNS preferentially. With this in mind, it becomes easier to interpret the conflicting reports. If an uncoupled NOS is inhibited via L-NNA, this will decrease ROS/RNS production, leading to decreased activation of proliferative pathways. Additionally we believe uncoupled NOS is the driver of tumor progression and maintenance, not a normally coupled NOS which produces NO. Another example of this is shown in examining S-nitrosylated proteins. S-nitrosylation occurs when NO reacts with the thiol group from a cysteine. Proteins are analyzed using the biotin switch method (See Chapter 2, materials and methods), however this method can also recognize other forms of oxidized cysteines (unless performed with ascorbate as the reducing agent, as was done in this study). These other oxidized forms of cysteine, such as sulfonic and sulfenic acid, are formed by peroxynitrite and superoxide molecules [79, 80], not NO. Thus as mentioned earlier, if NOS is uncoupled, the proteins detected by the biotin switch assay, may in fact be oxidized forms of cysteine, we believe the interpretation of these results has been another reason for the seemingly contrasting effects of NO.

In situations when NO donors are added cells with an uncoupled NOS generating O2-, this leads to the production of $ONOO^-$ leading to activation of proliferative and anti-apoptotic pathways. However, as the concentration of NO donors is increased, this

leads to increased DNA damage and other NO dependent pathways which have been shown to decrease proliferation. Thus viewed in light of NOS coupling, conflicting results can be better understood. Uncoupled NOS is a driver of tumor progression and maintenance, thus by recoupling NOS with SP, we can decrease proliferation *in vitro* in colorectal cells. We will next examine the effects of SP on *in vivo* tumors developed using a murine colitis associated colorectal cancer model.

Chapter 3:
Recoupling NOS *in vivo* and Mechanism of NOS Uncoupling in Colorectal Tumors

Introduction

The aims of the studies in this chapter are to use SP as a therapeutic agent for the treatment of colorectal cancer *in vivo* and to gain insights into mechanisms of NOS uncoupling. The previous chapter demonstrated that SP does have cytotoxic and anti-proliferative effects in CRC cells via a decrease in β-catenin levels and activity. Thus we hypothesized in this model of CAC, administering SP therapeutically after tumor formation, should decrease proliferation of these tumors.

Dextran Sodium Suflate (DSS) induced colitis and AOM induced colon cancer

As discussed, inflammation provides initiating and promoting stimuli and mediators, generating a tumor-prone environment. For my studies I use an established model for colorectal inflammation leading to colorectal tumors [91]. Initially, animals are treated with azoxymethane (AOM, carcinogen) and subsequently given 3, one week cycles of DSS (see Figure 3.1). In between the DSS cycles, animals are put on normal drinking water. Tumors start to form during week 8 of DSS treatment cycle. In this animal model, DSS provides the inflammatory environment while a single exposure to AOM provides the initiating event. In combination the latency period for tumor development is dramatically reduced. This method of spontaneous tumor generation in mice mimics very closely the pathophysiology of CAC in humans such as with UC or Crohn's Disease patients [91].

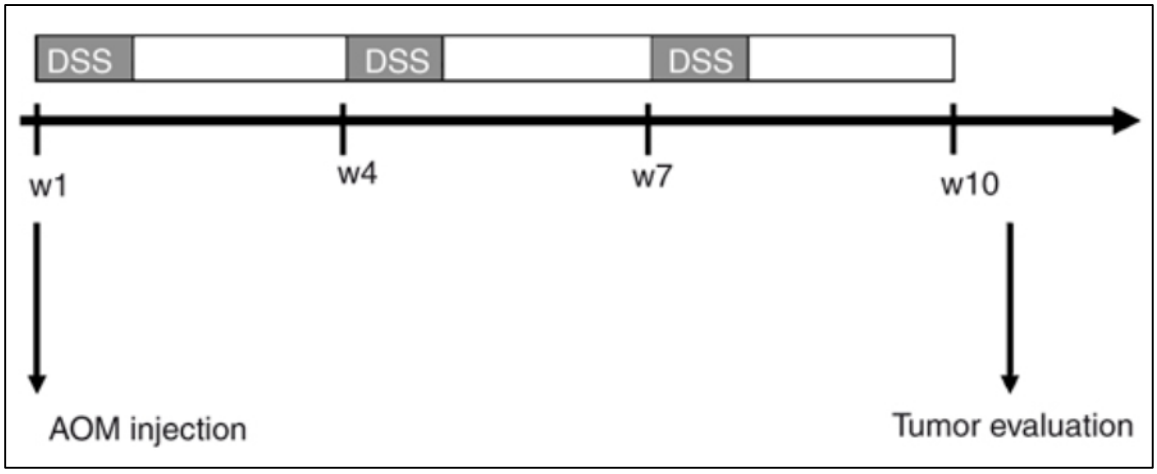

Figure 3.1: Azoxymethane and Dextran Sodium Sulfate Colitis Associated Colorectal Model. AOM is injected I.P. then the animals are started on three 1-week cycles of DSS. In between the cycles, normal drinking water is administered for 2 weeks, to allow for recovery from colitis. Tumors appear around week 8, but can vary.

Previous studies in our lab have shown that, prophylactically, SP was able to decrease the degree colitis (and associated symptoms such as weight loss, diarrhea as well as damage seen histologically to the epithelium and tumor burden. We saw a decrease in inflammatory cytokines such as IL-1 and IL-6, decrease in nitrotyrosine staining in SP treated tumors (a hallmark of oxidative stress) and diminished tumor burden in SP treated animals [53]. However in these studies, SP was administered prior to colitis induction, rather than after tumor development. Thus due to our *in vitro* data in colorectal tumor cell lines, we decided to implement SP treatment in this CAC model after tumors were detected using /PET/CT imaging.

For these studies we used FDG as the PET probe. Animals are starved overnight since FDG is preferentially accumulated in highly metabolically active tissues. Tumors (and inflammatory tissues in general) generally take up FDG very quickly, along with brain and the heart. Kidneys and bladder are the main excretory pathway, thus on a typical scan, the heart, brain and tumor sites, along with urogenital tract will be “hot spots” allowing for the 3D-visualization of these tissues. This non-invasive technique allows us to analyze initiation and progression of the tumors, as well as monitoring the therapeutic effects of SP and a surrogate marker for tumor volume calculated via the FDG hotspot [92]. Thus with the spontaneously generated tumors we will be able to analyze the effects of SP, much as clinicians do in patients, as well as use classical *ex vivo* techniques to confirm imaging results.

Potential Mechanisms of NOS Uncoupling

Another valuable component of this CAC model is our ability to separate intact non-tumor colonic epithelial cells from tumor tissue. We have adapted a protocol

developed by Nik et al. [93] which separates intact colonic epithelium from mesenchymal layers of the colon. This technique allows for separate analysis of the two layers. We use this same technique to first remove colonic epithelial cells and then excise tumors for our analyses. Using this technique we can determine molecular differences between the tumor cells and their non-tumor counterparts, within the same animals (much like when tumorigenic and normal tissues are biopsied from patients with colorectal cancer). This technique may provide insight into how and why NOS is uncoupled in colorectal tumors.

The question arises, how in fact do certain cells, such as myocytes after an infarct or tumor cells, become uncoupled. In myocytes, the answer may be a simple oxidation explanation, due to ischemia causing an increase in ROS/RNS and oxidation of BH4 to BH2 [94]. In this context, it is beneficial for myocytes which need to proliferate in order to survive the infarct. However after the infarct and ensuing inflammation mediated wound repair pathways are resolved, tissue homeostasis is restored and myocytes presumably return to a coupled state (unless of course a massive infarct occurred which caused death).

However, tumor cells and other chronic inflammatory conditions may be different. These cells must enact mechanisms to maintain an uncoupled state. One explanation may be the infiltrating inflammatory cells providing ROS/RNS (or other signals) to remain in an oxidative state or even the oxidative microenvironment itself. However this explanation doesn't account for the decreased BH4:BH2 we have measured *in vitro,* where these cellular components are lacking. Another component of the direct oxidation hypothesis may be an increase in ROS/RNS generating pathways, such as NADPH

Oxidases (NOX), within the tumor cells which perpetuates a low BH4:BH2 ratio [95]. Another possible mechanism maybe a molecular alteration in the BH4 metabolism pathway. These later two potential mechanisms can result in decreased BH4:BH2 ratios both *in vitro* and *in vivo.*

Tetrahydrobiopterin Synthesis and Recycling

BH4 synthesis and recycling is a well-regulated process dependent on many enzymes (Figure 3.2). Although there are several enzymes important in de novo synthesis and recycling of BH4, we have chosen to analyze four which are important in both pathways. GTP Cyclohydrolase-1 (GCH-1) is the enzyme responsible for catalyzing the rate limiting step in de novo synthesis. In previous work [42], we have shown that by over-expressing GCH-1 we are able to increase the BH4:BH2 ratio in MCF-7 breast cancer cells. Sepiapterin Reductase (SR, SPR) is an enzyme responsible for converting the final precursor of BH4, 6-Pyruvoyl Tetrahydrobiopterin to BH4 in the *de novo* pathway, but also converting BH2 (and SP) back to BH4 in the salvage pathway. Quinone Dihydropteridine Reductase (DHPR/QDPR) is also important in both the salvage and de novo pathways, much like SPR it is responsible for converting upstream pteridine derivatives into BH4. Lastly, GCH-1 Feedback Regulating Protein (GFRP) is an allosteric inhibitor GCH-1 [96]. There is evidence that in a variety of conditions, especially vascular endothelium dysfunction, alterations in pteridine metabolism causes altered recycling and *de novo* synthesis of BH4 [97-100]. Thus we hypothesized that these 4 proteins may be altered at the molecular level, resulting in decreased BH4 synthesis or decreased salvage of BH4 from BH2, leading to a decrease in BH4:BH2 ratio.

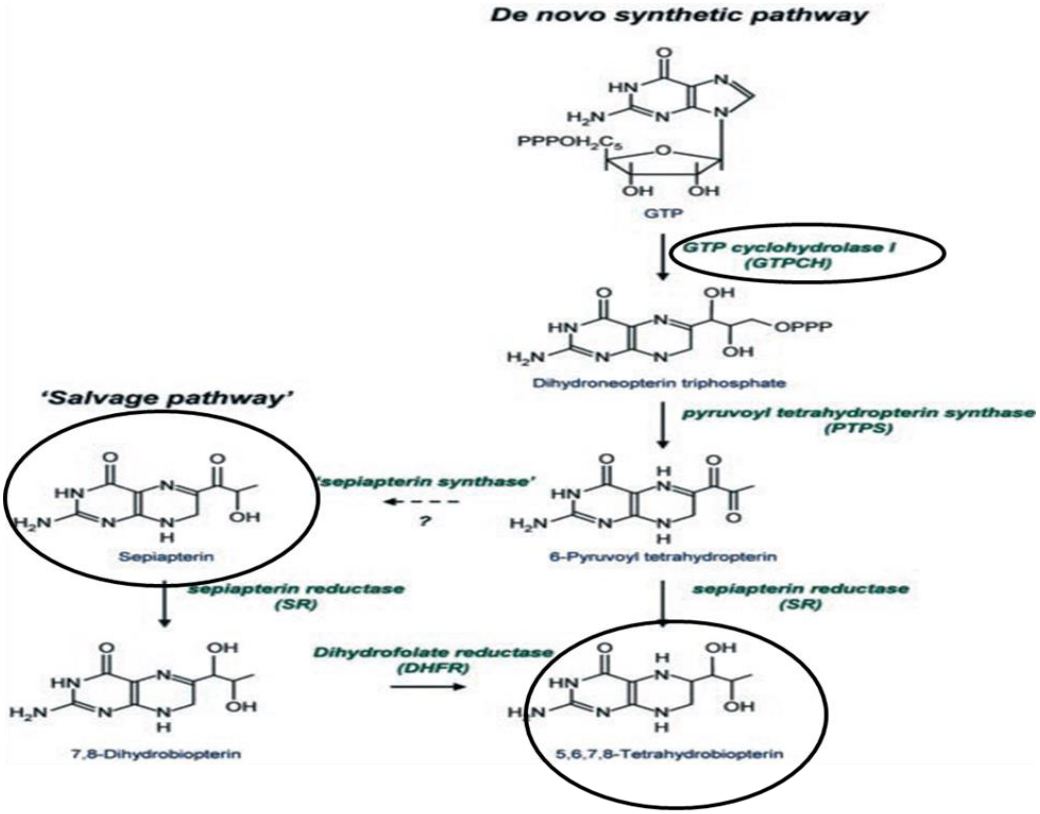

Figure 3.2: BH4 Biosynthsis and Salvage Pathways. The circled compounds are mechanisms by which researchers have shown can elevate BH4 levels in tissue culture or animals. Sepiapterin Reductase (SR) is an enzyme important in both the *de novo* and salvage pathway of BH4, as well as needed to convert exogenous SP into BH4

Thus the studies in this chapter sought to determine if SP has therapeutic benefits in spontaneous CAC. FDG/PET imaging was used to determine when tumors arise, then start treatment with SP and use *ex vivo* techniques to determine the effects of SP on spontaneous tumors in mice. Experiments were also conducted to determine a mechanistic explanation of decreased BH4:BH2 ratios in these colorectal tumor cells. Inhibitors of ROS/RNS generating enzymes and ROS/RNS scavengers were used to see the effects of ROS/RNS within the tumor cells on BH4:BH2 ratio. Lastly, expression levels of GCH-1, GFRP, QDPR and SPR (in both mouse tissue and human RNA data) to determine if there are differences in biopterin metabolizing enzymes in tumor cells compared with normal colonic epithelial cells. The combination of these two later studies provided plausible mechanisms for how NOS is uncoupled in colorectal tumors.

Materials and Methods

A. Mouse model of colitis and colorectal carcinoma

Long-term colitis/carcinogenesis was induced by the I.P. injection of AOM (10mg/kg) seven days prior to the onset of DSS treatment. Three, 5-7 days long each (depending on weight loss of animals), courses of 2% DSS were given as above separated by 2 weeks of DSS-free water. All animals were monitored daily for weight, stool consistency and the presence of blood in the excreta. Disease activity index (DAI) was determined by combining scores for weight loss, stool consistency and bloody excreta as follows: Weight loss (0: <1%, 1: 1-5%, 2: 5-10%, 3:10-15%, 4: >15%); Stool consistency (0: normal, 2: loose, 4: diarrhea); Blood in excreta (0: normal; 2: reddish, 4: bloody). Usually by day 5 on 2% DSS

animals lost ~10% of body weight and showed signs of gastrointestinal stress. Mice designated for SP treatment received either the long term SP course: 10mg/kg via drinking water for 3 weeks or short course: 3 daily doses for a total dose of 10mg/kg via oral gavage for 8 day treatment course. All animals were monitored daily for weight, stool consistency and the presence of blood in the excreta. All procedures were approved by the Institutional Animal Care and Use Committee of Virginia Commonwealth University and conformed to the guidelines established by the National Institutes of Health, protocol numbers AM10080 and AM10185.

B. Western Blot Analysis

Protein was extracted from flash frozen tumors excised from colons using a pestle and mortar in 20 ml/g tumor RIPA lysis buffer (50 mM Hepes pH 7.4, 150 mM NaCl, 1% Triton X-100, 1% sodium deoxycholate, 0.1% SDS, 5 mM EDTA) and processed under reducing conditions. Proteins were resolved by SDS-polyacrylamide gel electrophoresis and transferred to nitro-cellulose membranes. Membranes were incubated with the primary antibody of interest overnight at 4°C. Blots were developed using IR 700 or IR 800 conjugated secondary antibodies (Rockland Immunochemicals, Gilbertsville, PA) diluted 1:10,000 and imaged/analyzed using the Odyssey Licor system.

C. Histopathology and Immunofluorescence Staining

Colons were excised from animals, flushed with PBS, cut longitudinally, rolled into “swiss rolls” and immediately flash frozen in liquid N_2. Tumors were also

excised separately, rinsed in PBS and flash frozen. Frozen Swiss rolls or excised tumors were embedded in OCT and cryosections prepared.

For β-Catenin detection, frozen sections were fixed in ice-cold acetone for 10 min. After blocking with goat serum blocking for 60 min, the sections were stained with primary monoclonal antibody for β-Catenin (BD Biosciences Catalog #, 610154) overnight at 4^{o}C, followed by incubation with Alexa488-labeled goat anti-mouse secondary IgG (Invitrogen) at RT for 1 hour. A negative staining control was performed by incubation with isotype control Abs.

For Hematoxylin and Eosin (H&E) staining, cryosections (20 μm) were fixed in 4% paraformaldehyde, submerged in Modified Mayer's Hematoxylin (Richard Allan Scientific), destained in acid ethanol, stained with eosin, dehydrated and mounted with permount. Images were captured using the Ariol Digital Pathology Platform.

For ApoTAG Staining, a kit was purchased from Millipore (Catalog# S7111). Sections from excised tumors were fixed and stained according to the protocol accompanying the kit.

D. PET/FDG Image Acquisition and Analysis.

Fasted and anesthetized (2% isoflurane in Oxygen) animals were tail vein injected with 300 μCi [^{18}F]FDG from IBA Molecular, (Sterling, VA). After 60 minutes of FDG uptake, animals were positioned in the Inveon Preclinical System (Siemens Healthcare, PA) and PET/CT images acquired for 10 minutes with no attenuation correction. The PET images were processed using

manufacturer recommended calibration procedures and a phantom of known volume and activity acquired prior to the study. OSEM3D-MAP reconstructions were done using Inveon Acquisition Workplace 1.5 and were used for region-of-interest (ROI) analysis in the Inveon Research Workplace 4.1. The percent injected dose/gram of tissue (%ID/g) values were calculated after appropriate decay corrections using the formula, $\%ID/gm = C_t/ID \times 100$, where C_t is the concentration of radiotracer in the tissue (MBq/cc), obtained from the PET images after ROI analysis.

F. **Separation of intact colonic epithelial cells from mesenchymal layer**

Colons were excised (see chapter 3 section D). After cleansing and rinsing in PBS, the excised colon was carefully slid onto oral gavage needle with a 5cc syringe drawn with air. The distal end of the colon was slid on first, and the proximal end of the colon ended up at the tip of the needle. The proximal end was tied using surgical sutures at the tip. At the tied end, the colon was carefully inverted up on itself, until eventually the distal of the colon is now hanging off the needle, and the whole colon is inverted. The distal end is then tied off with suture. The colon is carefully inflated with air. In 15mL conical tubes, 1 mL of Cell Separation Solution (part number) is incubated on ice and the inverted, inflated colon is submerged in separation solution for 15 minutes. Every 5 minutes, the air is drawn from the balloon and the colon re-filled. After 15 minutes, the colonic villi are carefully scraped from the mesenchymal layer using a scalpel into cold PBS, allowing for analysis of separated epithelial cells.

G. RNA Isolation and qPCR Gene Expression Analysis

RNA from extracted colonic epithelia cells was obtained using RNeasy Kit from Qiagen and stored at -80º C. cDNA was made from the extracted RNA fresh on the day RT-PCR was to be performed using iScript cDNA Synthesis Kit from Bio-Rad and 1ug of RNA. Primers were made using Integrated DNA Technologies Primer Design Program for qPCR Assays (www.idtna.com) for SPR, GCHRF, GCH1, and QDPR. The sequences used for each are:

SPR For: 5’ CTGAGGAACCGAGTGTGC-3’ and Rev: 5’-CCCATCCGACTTCAACTTCTG-3’

GCHFR For: 5’-CATCAGCACTCAGATCCGTATG-3’ Rev: 5’-GGGTCGTTGACGTAGTATTCG-3’

GCH-1 For: 5’-GCATCACCTTGTTCCATTTGTAG-3’ Rev: 5’-AGGCGCTCTTGAACTTGTAG-3’

QDPR For: 5’-GTTGGAAAGCTCCTAGGTGAC-3’ Rev 5’-GTGGCTGGAGATAGTGGATG-3’

The primer sets were then ordered from Eurofins. Quantitative RT-PCR was performed using the FastStart Universal SYBR Green Master Mix RT-PCR Kit (Roche). 100 ng of cDNA was used for each 25 µl real-time RT-PCR reaction. The housekeeping GAPDH gene transcript was used to normalize mRNA gene expression. Real-time PCR was performed by a 7500 Fast Real-Time PCR System (Thermo Fisher Scientific). The PCR protocol conditions were as follows: 50°C hold step then 95°C for 10 min, followed by 40 cycles of 95°C for 15s and 60°C for 60s. A melting curve analysis was performed using the software’s SYBR green protocol to ensure no primer-dimer were made and the reactions were successful.

H. mRNA Analysis from Matched Tumor-Normal Colon Patient Samples

Log transformed data for tumors and their corresponding normal tissue expression data was obtained from The Cancer Genome Atlas (TCGA) Data Matrix. Mike Waters, (MD/PhD Candidate from Dr. Tomek Kordula's Lab) acquired and analyzed the data for this comparison.

Results:

Sepiapterin raises BH4:BH2 ratios *in vivo* leading to decreased tumor associated FDG activity and tumor size

After the final round of DSS, animals were placed back on normal drinking water for two weeks to allow for the symptoms of colitis to subside. After two weeks, a group of animals (N = 9) was treated with 10mg/kg SP for 3 weeks administered in drinking water, while control animals (N =10) were kept on normal drinking water. Animals were first imaged at the end of week 9 before any treatment and then subsequently every week. All animals were sacrificed at the end of week 13 (5 weeks after completion of last DSS round). We excised tumors from each group of animals to perform *ex vivo* analyses. We first wanted to measure BH4:BH2 ratios in this spontaneous CAC model, Figure 3.3 shows that indeed SP was able to raise the BH4:BH2 ratio almost 4 fold in our SP treated animals as compared to control tumors. We next examined gross differences in SP treated versus non treated animal colons. Figure 3.4 shows that SP treated animals had less tumors than control animals and relatively smaller tumors.

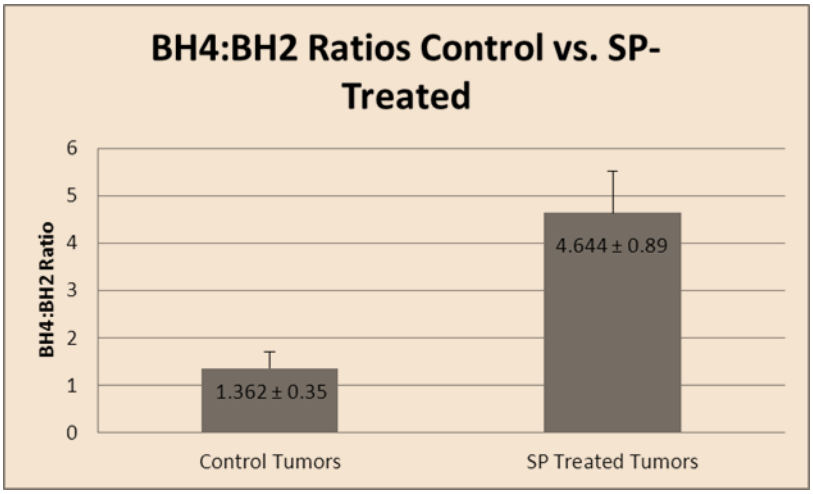

Figure 3.3: BH4:BH2 Ratios Measured in C57Bl/6J Mice with Spontaneously Generated CAC Tumors. BH4:BH2 Ratios were measured *in vivo* colorectal cancer tumors using HPLC. Animals were treated 10mg/kg/L in drinking water with SP for 3 weeks. Values are given ± SEM (N = 5 control animals and 5 SP treated animals).

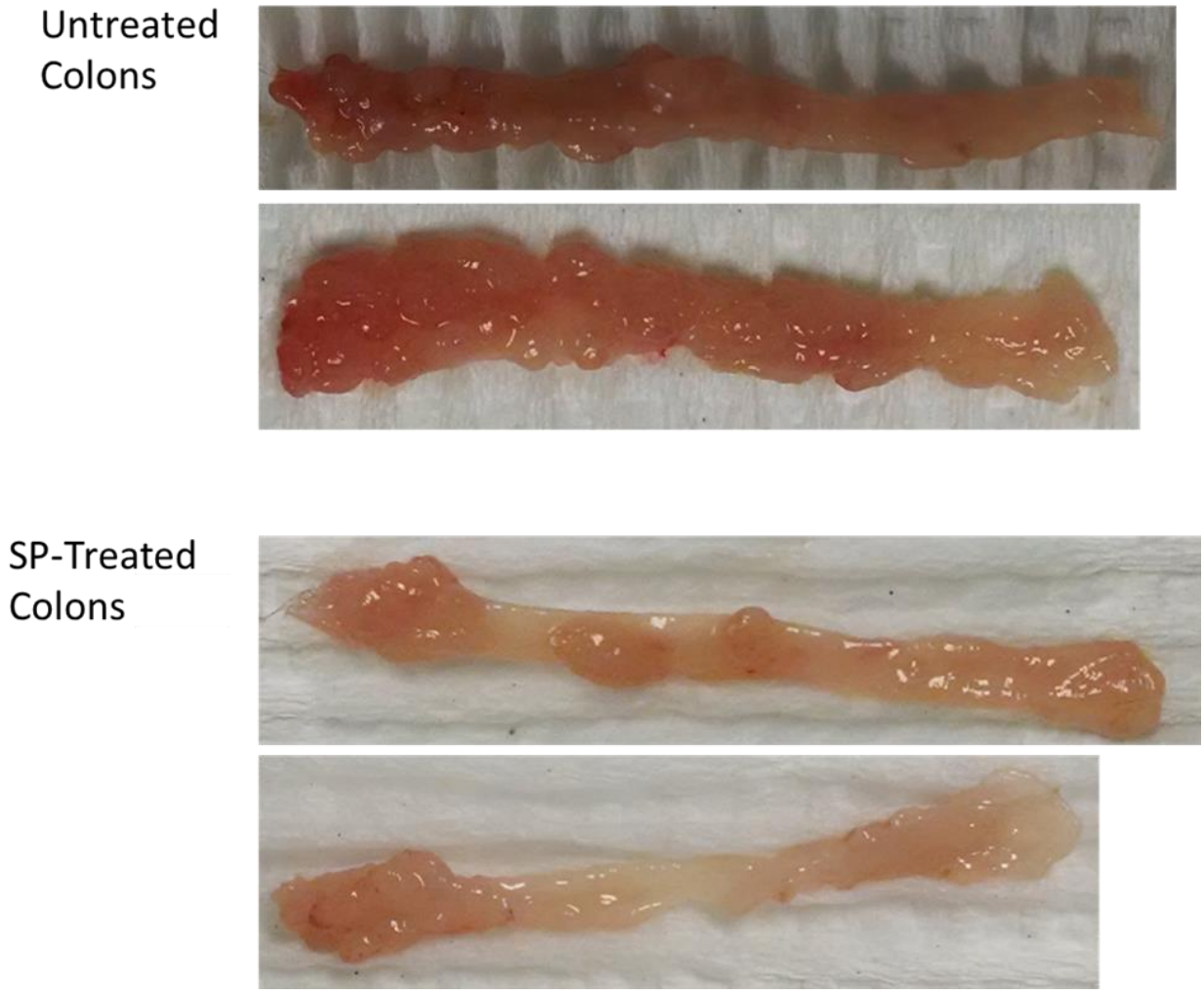

Figure 3.4: Gross comparison of SP Treated versus Non treated CAC Tumors. At 10 weeks post AOM injection (2 weeks post final DSS treatment) SP treated animals were administered with 10mg/kg/L in drinking water with SP for 3 weeks. Control and treated animals were sacrificed and colons harvested for tumor analysis. Although the effects of SP varied on tumor growth, overall SP decreased size and number of tumors when compared with untreated animals. Representative images are shown (N = 5 control animals and 5 SP treated animals)

The tumors in control animals were also visually redder (possibly more inflamed) in color when compared to SP treated animals. Lastly, we observed that SP treated colonic tissue was less fragile that control tissue, control colons were easily torn during dissections. We next sought to corroborate what we had seen on gross dissection with FDG/PET images we had acquired of the SP treated and control animals. Figure 3.5A shows the results from 3 SP treated and control animals after two weeks of SP treatment. The numbers in parentheses represent FDG uptake from our colonic tumor regions of interest, pre and post SP treatment. Figure 3.5B is the cumulative change in FDG uptake between week 9 and week 11 (2 weeks post SP treatment). Control animals show about a 50% increase in FDG uptake in that two week time span, whereas SP treated animals show 25% decrease in FDG uptake in the same time span. Thus SP treatment at two weeks was able to decrease FDG uptake. In this animals, SP was administered in the drinking water, however this made the exact amount of SP each animal received nearly impossible to measure. We also realized the need to measure FDG uptake at an earlier time point. We decided to address these issues by administering SP treatment via oral gavage, 3 times daily for only 8 days. In this treatment course we again used FDG/PET to follow tumor growth and drug effect. We scanned 10 animals at week 12, then again at week 14, then 3 days into SP treatment and a final scan at 8 days of SP treatment. Figure 3.6A shows FDG/PET images of two representative animals. The red rectangles represent tumor regions of interest that we followed during the treatment course. Figure 3.6B shows before SP treatment, FDG uptake increased almost two fold from baseline, but after 3 days of SP treatment there was about a 30% decrease in FDG uptake from baseline

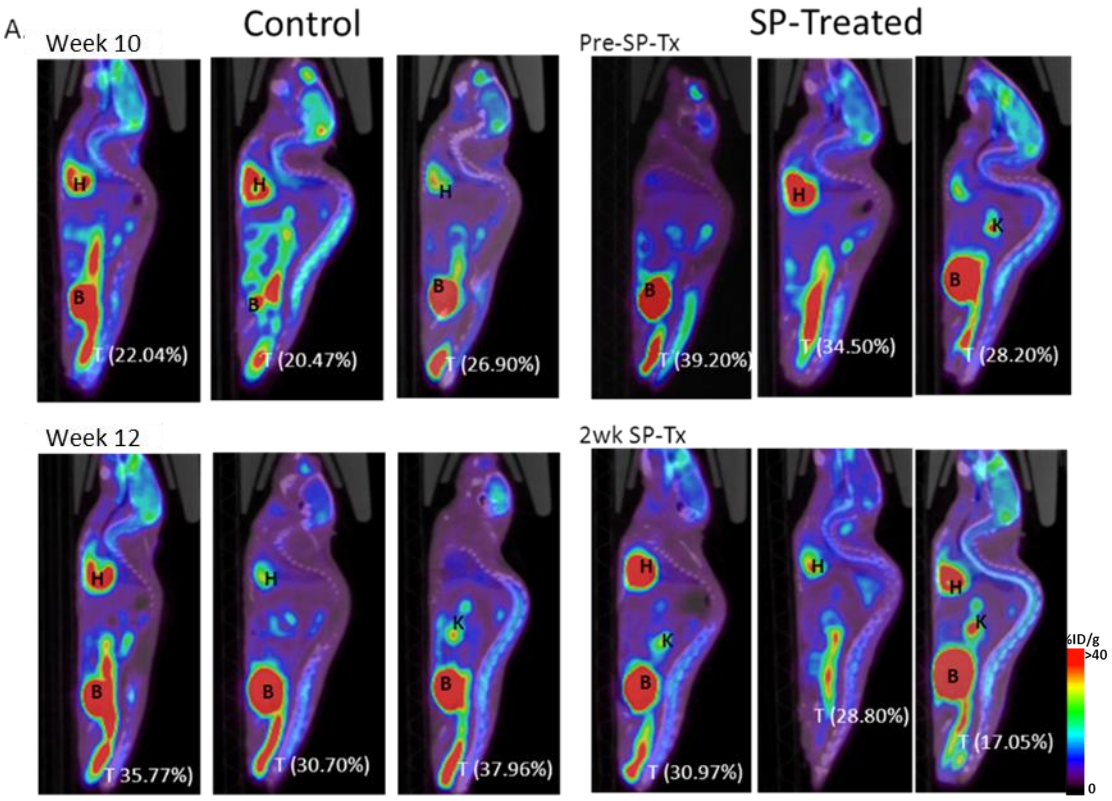

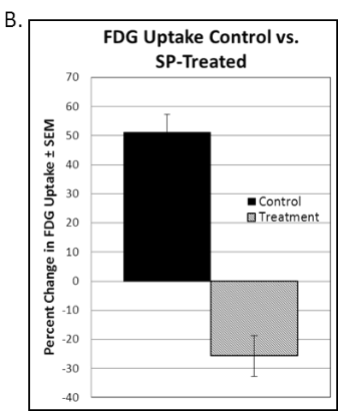

Figure 3.5: FDG/PET Images of C57Bl/6J Mice with long term SP Treatment. At 10 weeks post AOM injection (2 weeks post final DSS treatment) SP treated animals were administered with 10mg/kg/L in drinking water with SP for 3 weeks. Animals were imaged weekly and tumor progression was followed. A) Images are from 3 animals in each group at week 9 and again after 2 weeks of SP treatment. *(H= Heart, K = Kidneys, B = Bladder, T = Tumor region of interest)* B) FDG Uptake values were calculated and the percent change from baseline was calculated and averaged (also shown in parenthesis in (A) images). These values show a decrease in uptake values in SP treated animals, while control animals increased FDG uptake in that time span. (N = 5 control animals and 5 SP treated animals)

A.

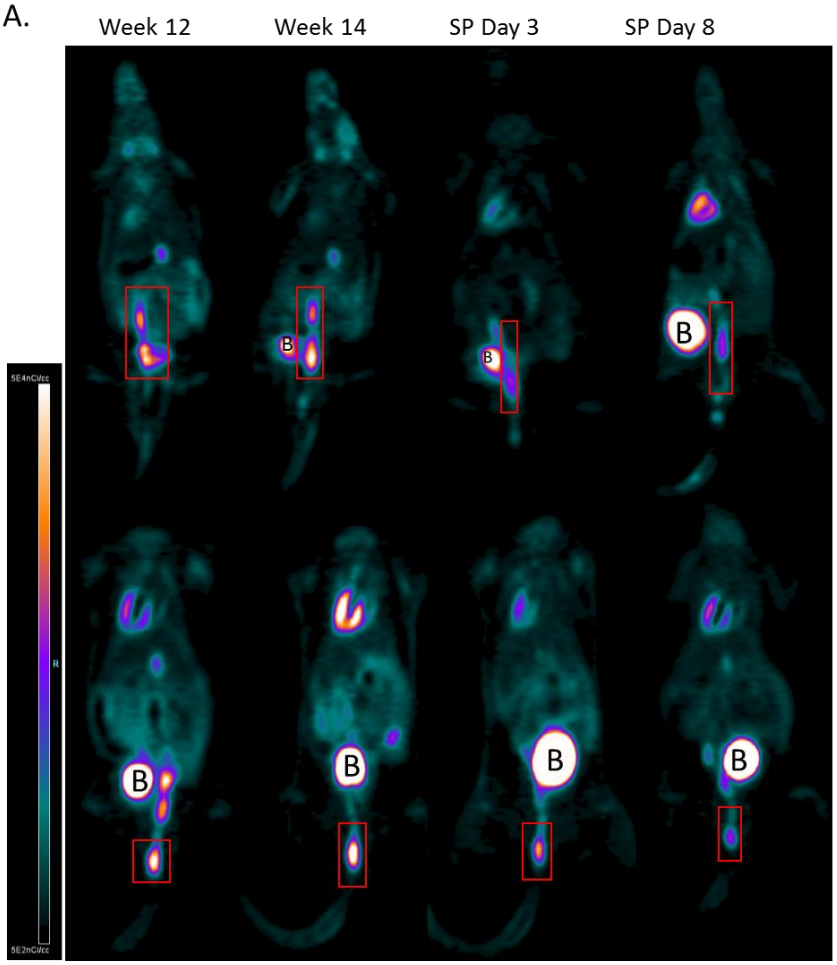

B.

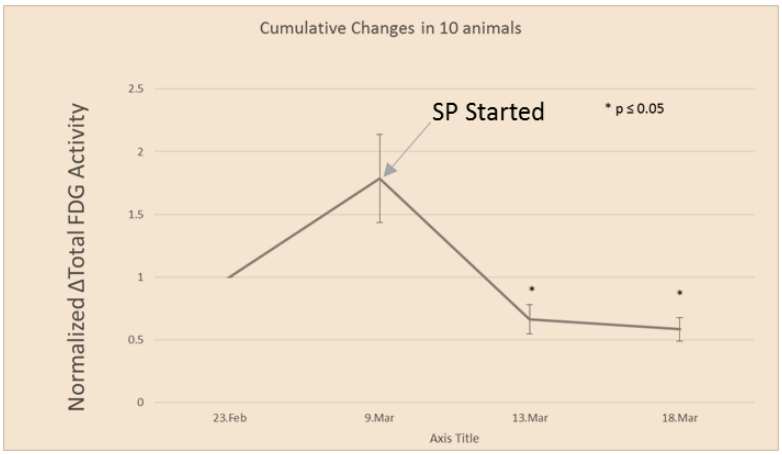

Figure 3.6: FDG/PET Images of C57Bl/6J Mice with short term Oral Gavage SP Treatment. At 10 weeks post AOM injection (2 weeks post final DSS treatment) SP treated animals were administered with 3.33 mg/kg/L 3 times/day for 8 days. Animals were imaged 2 times before SP treatment, then after 3 days and 8 days of SP Treatment. *(Red rectangle outlines tumor region of interest, B = Bladder)* B) FDG Uptake values were calculated and normalized to the fold change from week 10 and averaged for N = 10 animals. Fold change values are shown with ± SEM. * $p \leq 0.05$ using Student t-test was calculated between 9Mar FDG uptake and 3 or 8 days of SP treatment.

which was sustained at day 8 as well. When compared with our earlier two week SP treatment data (Figure 3.3) the shorter term oral gavage treatment efficacy is very similar. However, with oral gavage the exact amount of SP given to each animal is known and all animals showed a decrease in FDG uptake after 3 and 8 days of SP treatment. These data also show that, short term SP treatment has about the same efficacy as longer term treatment.

Sepiapterin leads to increased apoptosis and decreased β-Catenin expression in CAC tumors

We next sought to correlate our imaging and gross results with *ex vivo* analysis of excised CAC tumors that were treated with SP in drinking water for 3 weeks. We first examined apoptosis using the ApoTAG kit from Millipore. Figure 3.7A shows representative tumor sections from control and SP treated animals. SP treated animals showed an increase in apoptosis when compared with control animals. Figure 3.7B is the quantification for apoptosis staining in these tumors. We next sought to corroborate our *in vitro* findings with SP treatment and its effects on β-catenin expression. In *in vitro* experiments, SP treatment led to decreased β-catenin expression and Figure 3.8 shows that SP treatment led to decreased β-catenin expression both in tumor sections and tumor homogenates via western. Thus we have seen that SP leads to decreased β-catenin expression both *in vitro* and *in vivo*. Lastly, we sought to determine if SP has any effects on the expression of Vimentin. Vimentin is an important marker of the epithelial to mesenchymal phenotype tumor cells undergo as the tumor progresses from a differentiated cell to a more malignant cell. We again used our 3 week treated SP treated tumor sections. As seen in Figure 3.9, after treatment with SP for 3 weeks,

A.

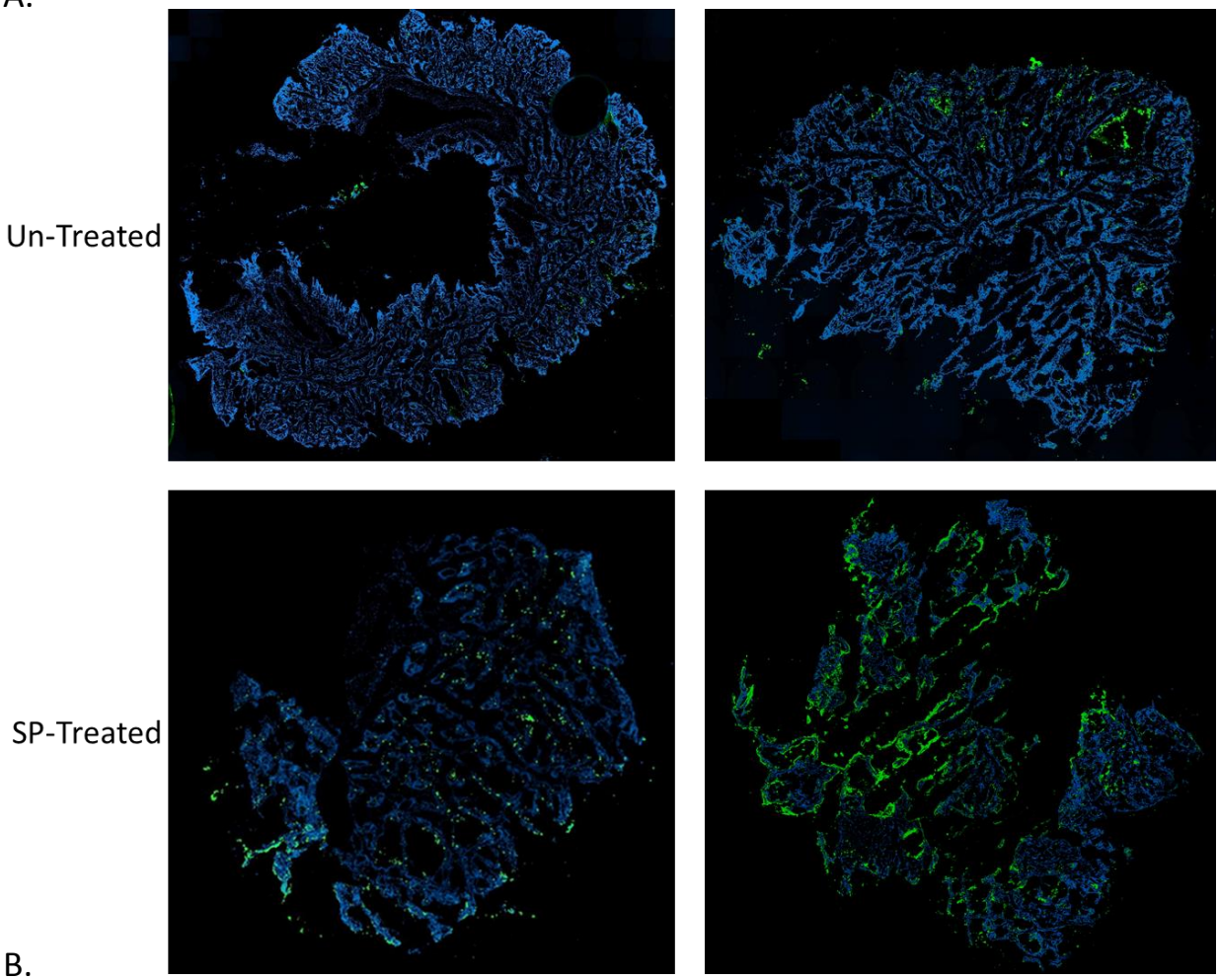

B.

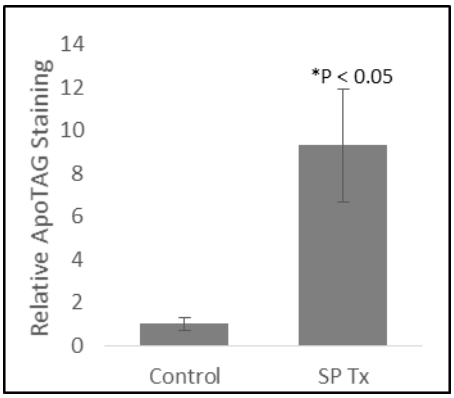

Figure 3.7: *Ex Vivo* Analysis of Apoptosis in CAC Tumors. At 10 weeks post AOM injection (2 weeks post final DSS treatment) SP treated animals were administered with 10mg/kg/L in drinking water with SP for 3 weeks. After treatment, animals were sacrificed and their colons removed. Tumors were excised from colon and histological slides were made and stained using ApoTAG Kit from Millipore. A) Representative sections are shown, with ApoTAG staining in green and Hoescht stain for nuclei in blue. B) Quantification was done by obtaining green:blue ratios (green ApoTAG staining to blue nuclei staining to account for size differences in tumors). Ratios were then averaged within Control (N =5) and SP treated animals (Tx) (N = 4) groups. Averaged ratio of controls was normalized to 1 and fold change was compared to SP treated animals. Values are shown ± SEM, * $p \leq 0.05$.

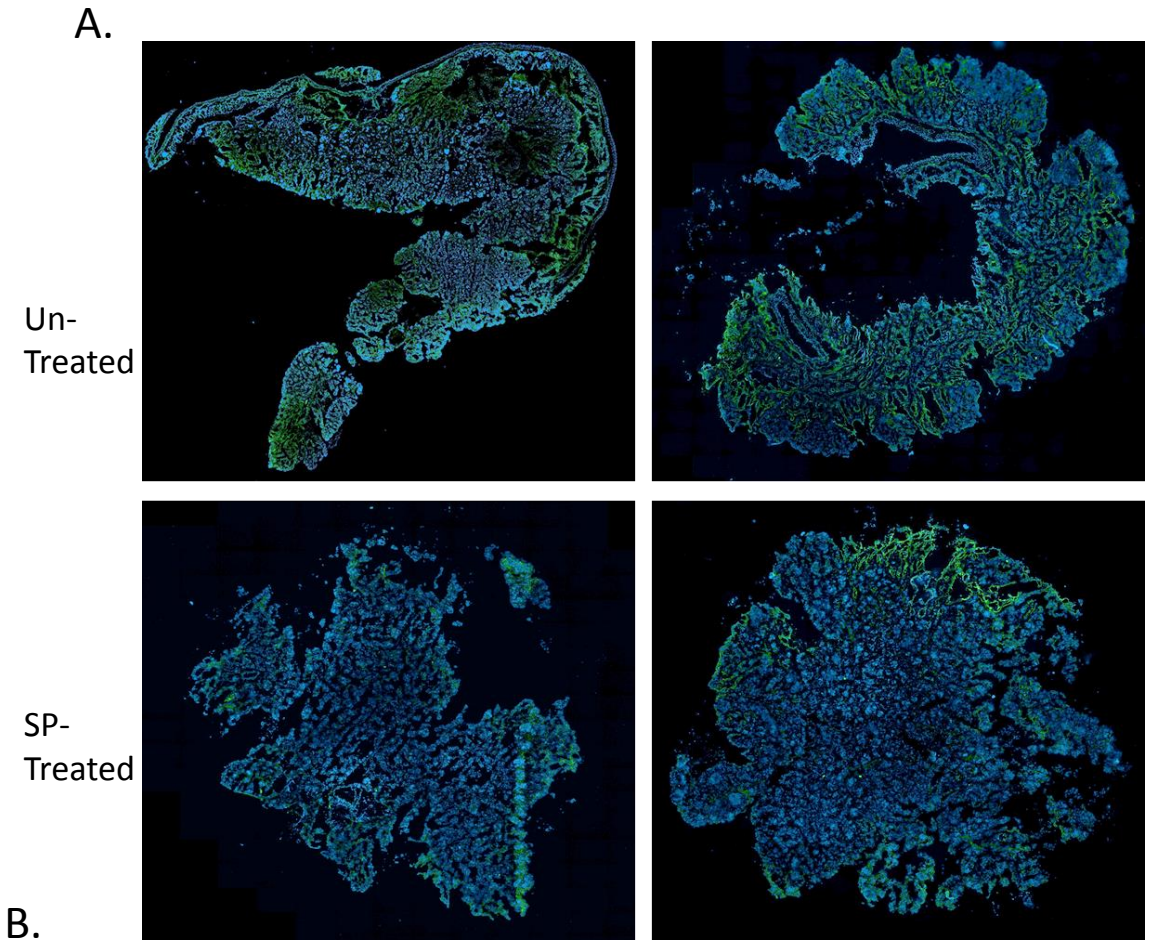

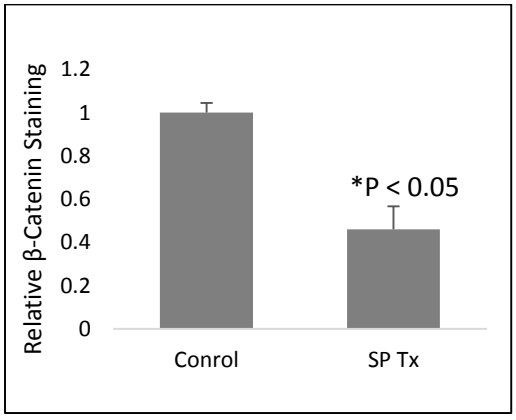

Figure 3.8: *Ex Vivo* Analysis of β-catenin in CAC Tumors. At 10 weeks post AOM injection (2 weeks post final DSS treatment) SP treated animals were administered with 10mg/kg/L in drinking water with SP for 3 weeks. After treatment, animals were sacrificed and their colons removed. Tumors were excised from colon and histological slides were made and stained using for β-catenin expression. A) Representative sections are shown, with β-catenin staining in green and Hoescht stain for nuclei in blue. B) Quantification was done by obtaining green:blue ratios (green β-catenin staining to blue nuclei staining to account for size differences in tumors). Ratios were then averaged within Control (N =5) and SP treated animals (Tx) (N = 4) groups. Averaged ratio of controls was normalized to 1 and fold change was compared to SP treated animals. Values are shown ± SEM. C) Western blot analysis, whole tumor homogenates from control or SP treated animals were analyzed for β-catenin expression levels.

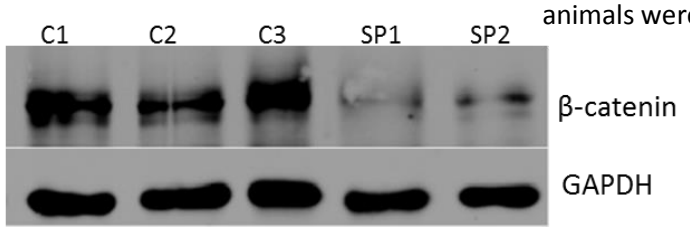

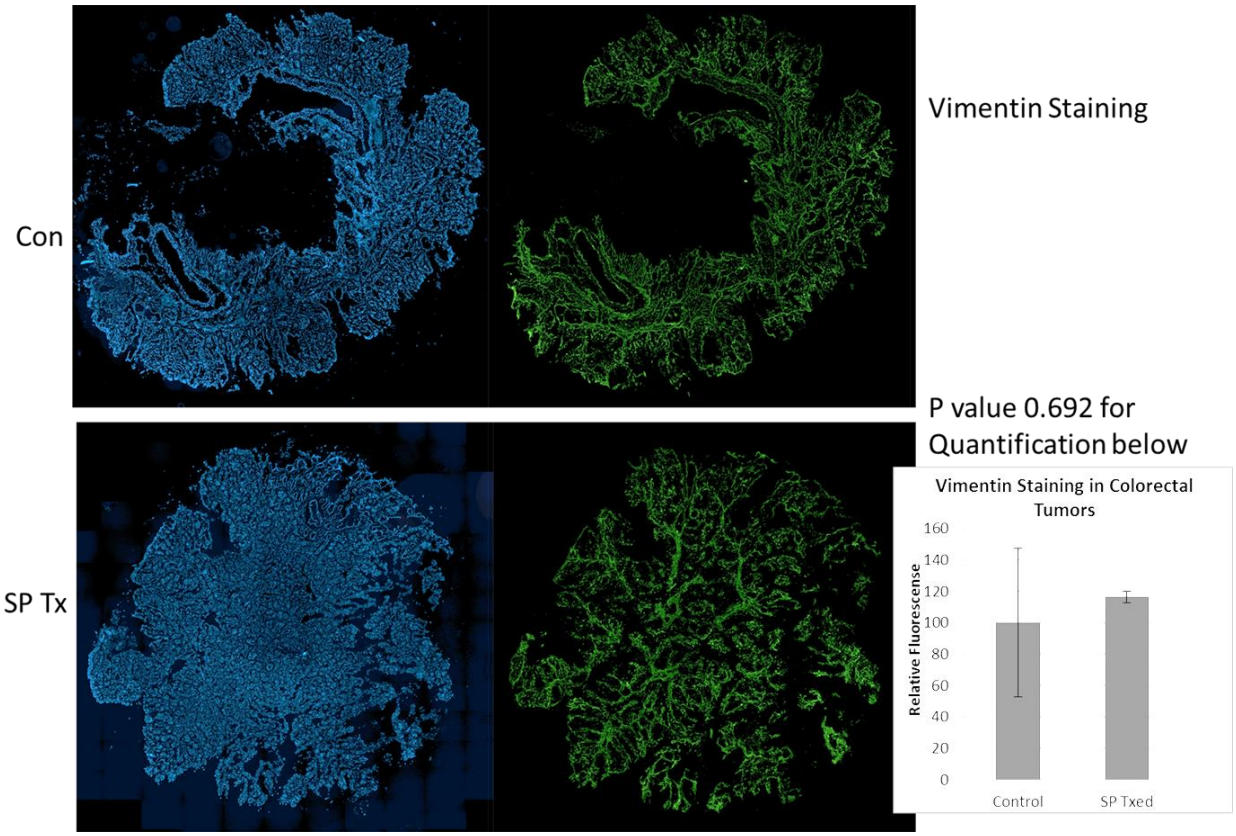

Figure 3.9: *Ex Vivo* Analysis of Vimentin CAC Tumors. At 10 weeks post AOM injection (2 weeks post final DSS treatment) SP treated animals were administered with 10mg/kg/L in drinking water with SP for 3 weeks. After treatment, animals were sacrificed and their colons removed. Tumors were excised from colon and histological slides were made and stained using for Vimentin expression. A) Representative sections are shown, with vimentin staining in green and Hoescht stain for nuclei in blue. B) Quantification was done by obtaining green:blue ratios (green vimentin staining to blue nuclei staining to account for size differences in tumors). Ratios were then averaged within Control (N =5) and SP treated animals (Tx) (N = 4) groups. Averaged ratio of controls was normalized to 1 and fold change was compared to SP treated animals. Values are shown ± SEM. C) Western blot analysis, whole tumor homogenates from control or SP treated animals were analyzed for β-catenin expression levels.

vimentin expression was not visually or statistically different between treated or control animals.

An oxidative environment and altered levels of biopterin metabolizing enzymes contribute to a decreased BH4:BH2 ratio

We first wanted to compare the levels of important enzymes in both the *de novo* synthesis and salvage of BH4 in normal colonic epithelial cells from non-tumor bearing animals with tumors from animals treated with AOM/DSS. Figure 3.10A is qPCR analysis of GCH-1, GRFP, QDPR and SR. After normalization to GAPDH mRNA and quantification, we saw that there were significant differences in GCH-1 and SR mRNA levels. GCH-1 mRNA was greatly upregulated, whereas SR mRNA was decreased. We next sought to correlate our transcript analysis with protein analysis using western blots in the same tumor tissues and normal colonic epithelial cells. Figure 3.10B shows western blot analysis of the four molecules. The first obvious fact is there is great variability from one tumor to the next. This is most likely due to this model of spontaneous tumor development, and the heterogeneity of the tumors within and across animals. These tumors arise at different times during the DSS treatment course, thus are at different stages. Aside from that fact, the western blot data does not seem to fit with our qPCR analysis very well either. It seems protein levels of QDPR are decreased in the tumors, whereas mRNA levels of QDPR are unchanged. Proteins levels of SR are elevated in tumor tissue, whereas the mRNA levels of SR were significantly decreased. In two tumors, GCH-1 levels are elevated, whereas in another two they are not. Lastly, GRFP protein levels seem to be decreased when compared with normal epithelial tissue. A caveat with this data is that the qPCR uses 10 tumors and 5 normal epithelial

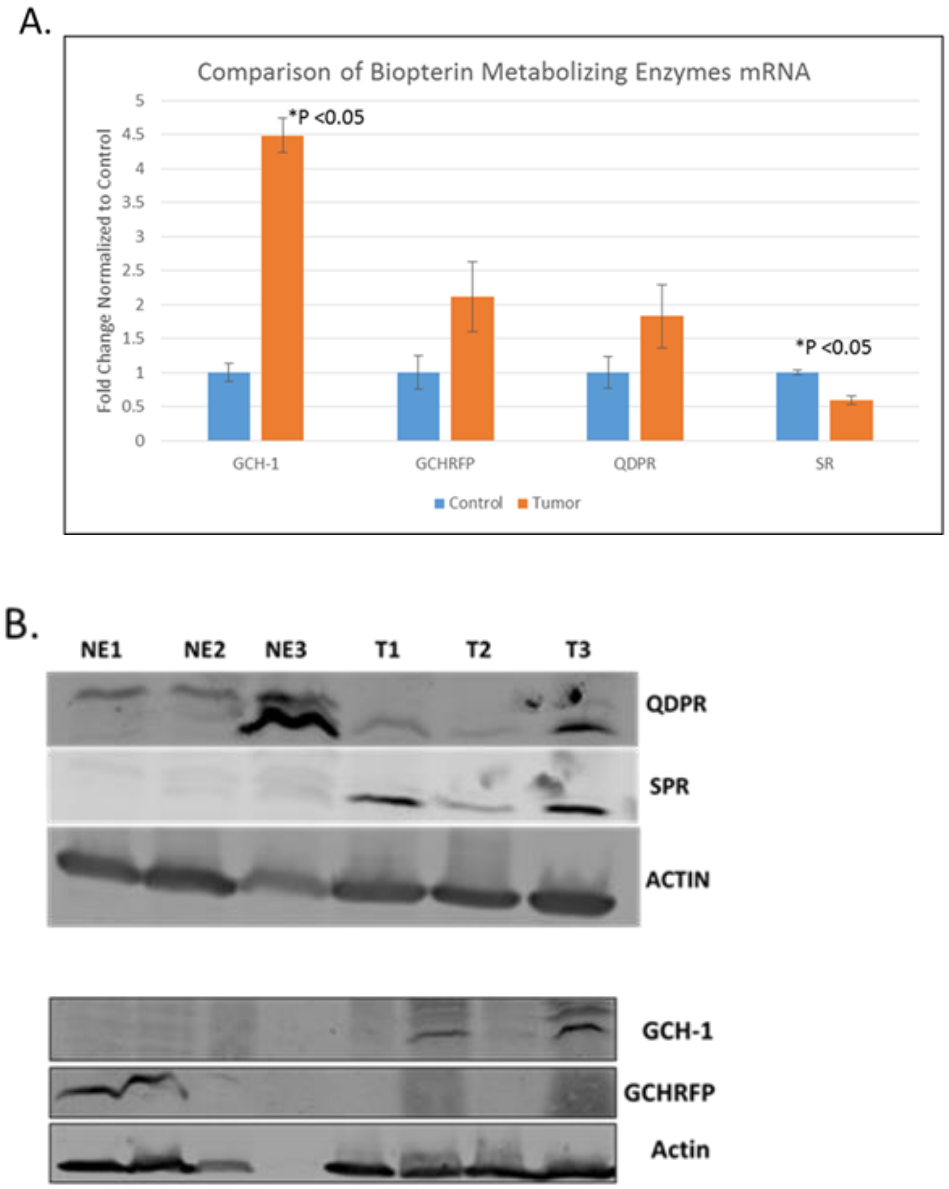

Figure 3.10: Expression Analysis of Biopterin Metabolizing Enzymes in C57Bl/6J Mice with CAC Tumors. Using the colonic epithelium separation technique, we separated normal epithelium (NE) and Tumors (T) from AOM/DSS treated animals. RNA and Proteins were extracted from NE and T from 3 animals (two tumors from animal 3 were used) A) qPCR was conducted to analyze for transcript levels of GTP Cyclohydrolase 1 (GCH-1), GCH Regulating Factor Protein (GCHRFP), Quinone Dihydropteridin Reductase (QDPR) and Sepiapterin Reductase (SPR, SR) Values are normalized to GAPDH levels and shown ± SEM. B) Western blot analysis of the same four enzymes.

tissue samples, whereas the western blot analysis uses tumors and normal tissue from 3 animals each.

We next sought to analyze these same four enzyme mRNA levels in tissue samples from human patients using The Cancer Genome Atlas's (TCGA) database. We compared normal colonic tissue expression and tumor tissue levels of these 4 molecules. In this analysis, (Figure 3.11) we saw only two of the four molecules had significant differences between normal and tumor tissue. GFRP mRNA levels were significantly increased and SPR levels were significantly decreased. Although it is not possible to correlate mRNA levels with protein levels in these samples, if we assume GFRP levels are increased this would inhibit GCH-1 and decrease BH4 *de novo* synthesis. If Sepiapterin Reductase levels are decreased, this would decrease recycling of BH2 back to BH4 via the salvage pathway (also decrease *de novo* synthesis because SR catalyzes a step in that pathway as well). Thus the end result of the change in enzyme levels of these two molecules will lead to decreased BH4 levels and a concomitant increase in BH2 levels.

In order to assess the effects of ROS/RNS generating mechanisms within the colorectal tumor cells, we used inhibitors and scavengers of ROS/RNS to determine their effects on BH4:BH2 ratios. L-NG-nitro-L-arginine (LNNA) is a specific inhibitor of NOSs, GP91 is a small peptide inhibitor of NADPH Oxidases, which generate superoxide molecules and EUK134 is a scavenger of superoxides and peroxinitrite. Table 3.1 shows the effects of BH4:BH2 ratio using these inhibitors of ROS/RNS alone and in combination. In all cases there was a slight increase in the BH4:BH2 ratio

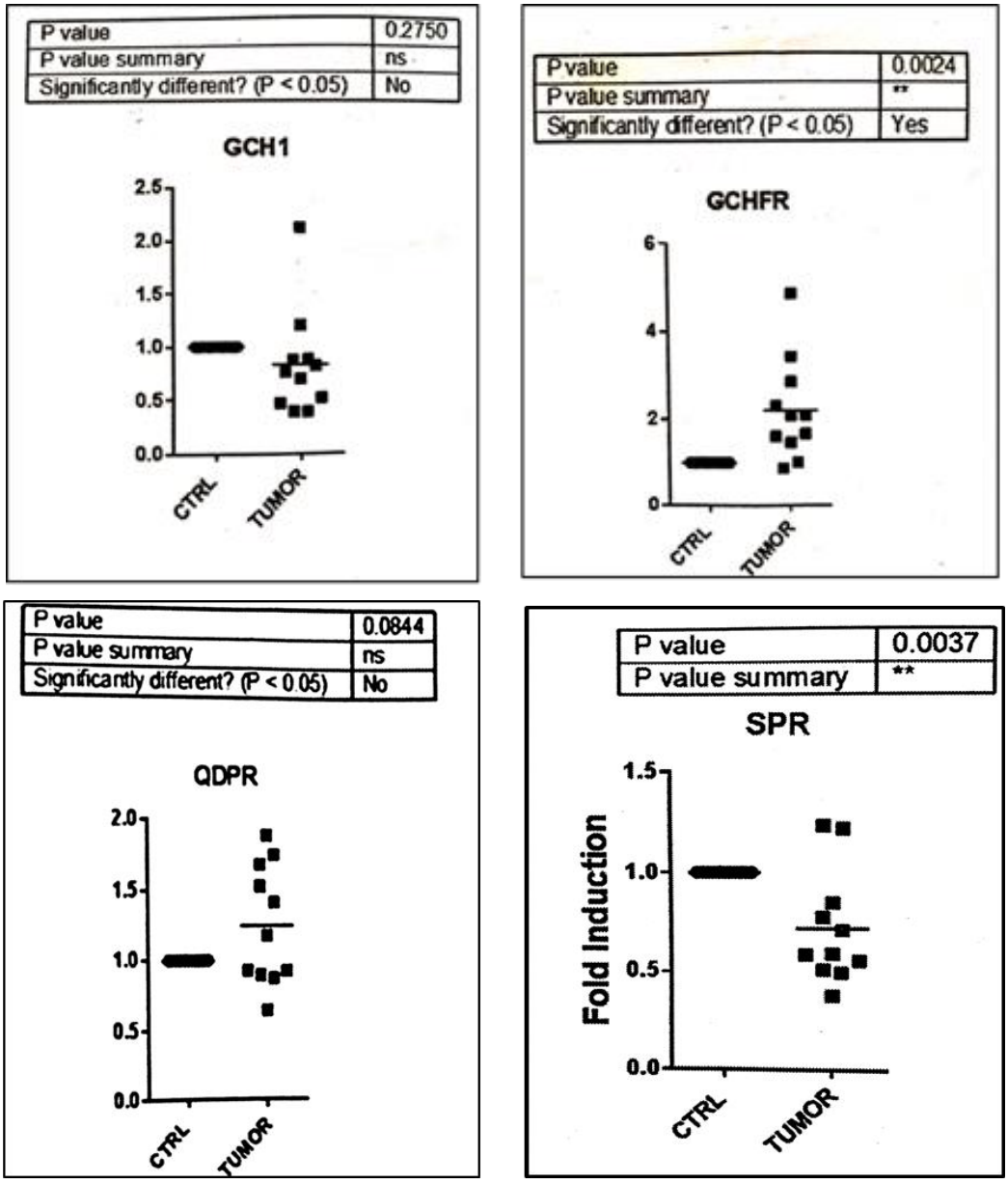

Figure 3.11: Expression Analysis of Biopterin Metabolizing Enzymes in Human Colorectal Samples and normal colonic tissue. Using The Cancer Genome Atlas (TCGA) database we obtained expression data from patients with colorectal cancer who had biopsies of colorectal tumors with expression data for normal colonic tissue in biopterin metabolizing enzymes.

	BH4:BH2 Ratio
Normal Colon Tissue	7.1 ± 0.6
Control HCT116 Cells	2.3 ± 0.2
LNNA	2.9 ± 0.1
EUK134	2.8 ± 0.1
GP91 NOX Inhibitor	2.7 ± 0.1
GP91 + EUK134 + LNNA	3.1 ± 0.3

Table 3.1: BH4:BH2 Ratios after inhibition of sources of ROS/RNS. Comparison of BH4:BH2 ratios after treatment of HCT116 cells with specific inhibitors of ROS/RNS. L-NG-nitro-L-arginine (LNNA) was used to inhibit NOS, 200nM for 24 hours. EUK134, Superoxide Dismuatase Mimetic, was used at 10uM for 24 hours. GP91, NOX inhibitor, used at 5uM for 3 hours. Values are given ± STD.

when compared to untreated HCT116 cells, with the greatest increase when all three molecules were used together.

Discussion:

The first section of this chapter focused on examining the effect of SP treatment had in animals which had undergone spontaneous colorectal tumor development. SP treatment in mice with colorectal tumors led to an increased BH4:BH2 ratio, signaling towards a coupled NOS. In both short term oral gavage therapy and long term SP in drinking water, we saw decreased FDG uptake, a surrogate marker for metabolic activity. On gross examination we saw decreased tumor size and number in treated animals. *Ex vivo* analysis showed that SP treatment increased apoptosis and a concomitant decrease in β-catenin expression levels. We did not see a decrease in vimentin expression, a marker for epithelial to mesenchymal transition (EMT). Due to the loss of β-catenin expression, we believe the mechanism to be similar to what was seen *in vitro* (Chapter 2). SP treatment leads to a recoupling of NOS (due to the increase in BH4) which leads to an increase in NO. This would shift the cellular signaling from proliferative/anti-apoptotic pathways which rely on superoxide and peroxinitrite, towards NO mediated pathways. As shown by our earlier work and others, NO can S-nitrosylate AKT leading to a decrease in its activity. Loss of AKT activity will lead to increased GSK3β activity and a decrease in β-catenin expression levels. AKT also regulates many other cellular metabolic pathways, such as glucose uptake into cells [101, 102]. Thus one reason for the decrease in FDG uptake (along with a decrease in tumor size and number seen on gross examination) may be decreased AKT activity causing decreased GLUT4 translocation. The loss of AKT activity leads to

decreased proliferation and increased susceptibility apoptotic signaling. Thus we believe that SP in combination with ionizing radiation (IR) can have radio-sensitizing effects on tumor cells. Preliminary work in our lab has shown that indeed, SP in combination with IR can be more cytotoxic than just IR or SP alone. However, due to its antioxidant effects, SP cannot be present during radiation treatment. We are currently working to determine the most efficacious treatment schedule of SP and IR. We also noticed that after 3 weeks of SP treatment, the response to SP seems to diminish with prolonged exposure, another reason to combine SP with other chemotherapeutic drugs and/or IR.

In our prolonged SP treatment, we also noticed variable response to SP treatment. Some animals responded very well to treatment, whereas others only saw a plateauing effect on FDG uptake. Upon gross examination, the tumors from SP treated animals were smaller and less in number but this varied from animal to animal. Thus we decided to treat animals via oral gavage with 3 daily doses of SP. This would address the potential problems that some animals received more SP than others and the difficulty to know exactly how much SP each animal received when SP was delivered through the drinking water. However, even with oral gavage delivery of the same dosage of SP to all animals and with all animals demonstrating a decrease in FDG uptake (although the time points were 3 and 8 days) the overall response still varied. One explanation may be due to differences in SR levels, as seen in Figure 3.8B. We saw varying amounts of SR levels thus SP is metabolized to BH4 differently in each of these tumors. It is important to stress that due to the heterogeneous nature of this model, the tumors are all at different stages of development, which may have an effect

on response. In our short term treatment course, we see that SP's greatest effect was after 3 days of treatment, which would have been missed with the longer treatment course. This may also explain the lack of effect of vimentin expression. Perhaps SP changes EMT markers early in the treatment and over time the tumor is able to become more resistant to SP. We measured vimentin expression in tumors which had been treated for 3 weeks. Current studies are underway in our lab to examine SP's effect on EMT markers as well as vascularization in shorter SP treatment course in CAC. Future studies are also underway to determine NOS uncoupling in infiltrating immune cells in the tumor microenvironment. Specifically we wish to analyze the coupling state of tumor associate macrophages (TAM) which play important roles in providing cytokines and growth factors to allow for maintenance and progression of the tumors. A strength of our DSS/AOM colorectal cancer model is that we can follow progression of the tumors and monitor the effect of inflammatory cells on tumor growth and development. iNOS is resistant to uncoupling via a drop in BH4:BH2 ratio [34] however can be uncoupled due to a decrease in arginine levels. Another important finding has been zinc ion levels can affect iNOS function and expression in a variety of immune cells. Zinc levels also play roles in NO availability and elevated levels can lead to apoptosis. Perhaps by recoupling NOS zinc levels are altered and can lead to apoptosis in tumor cells, as well as activate the immune cells against the tumor cells [103].

In this chapter we also sought to determine possible mechanisms of how the BH4:BH2 is altered in tumor cells. In order to determine possible mechanisms of a decrease in BH4:BH2 ratio, we used inhibitors for NOS, NOX and scavengers of ROS/RNS, as well as changes in expression of enzymes involved in biopterin

metabolism We analyzed mRNA and protein levels of 4 proteins important in the *de novo* and salvage synthesis of BH4 in both normal colon epithelial cells as well as tumor cells from tumor bearing animals. Using this spontaneous CAC model, we saw increased GCH-1 mRNA levels, decreased SR mRNA levels. QDPR and GFRP mRNA were not significantly different between normal and tumor tissue. Next we analyzed protein expression using western blot, hoping to corroborate our mRNA data. Instead we saw, in general, an increase in SR in tumor tissue (although there was variable amounts of SR in each tumor), decreased GFRP in tumor tissue, similar amounts of QDPR (although the protein may be of different size in the different tissue type) and varying amounts of GCH-1 between the 4 tumors. One possible explanation for the increased GCH-1 and SPR and reduced GFRP expression levels is that this is the futile response of the tissue to maintain a high BH4:BH2 under chronic inflammatory conditions. While I have shown with inhibitors of NOS and NADPH oxidase that ROS generated from these activities contribute to the low BH4:BH2 they by themselves remain insufficient to completely account for low BH4:BH2. Planned experiments will measure the enzymatic activities of GCH1, SPR and QDPR. We also plan to measure expression levels of cellular adhesion proteins (e.g. VCAM-1) that may facilitate recruitment of inflammatory cells to the colon and whether SP treatment by inhibiting NFκB activity reduces cellular adhesion protein expression or whether reducing inflammatory cells with for example anti-GR1+ to deplete animals of neutrophils will more substantially enhance BH4:BH2. Finally, one major concern, is the small number of animals we used to conduct this experiment. We are currently treating another batch of animals to conduct a more thorough study. Another concern is that the tumors in

these animals are heterogeneous and arise at different time points, thus some may be relatively “younger” whereas others may have arisen much earlier. There is considerable difference in their sizes as well. Thus this model may not be the ideal model to study biopterin metabolizing enzyme differences. We also plan to conduct similar experiments in MMTV mice which develop breast carcinomas and compare with normal mammary fat pad tissue with tumor tissue. There may also be post transcriptional regulation of the mRNA transcripts in tumor tissue, which may account for the differences seen via western blots. Another factor which must be considered in future studies is also the relative activities of these molecules in tumor tissue versus normal epithelial cells. The activities of these enzymes may also be perturbed, with or without a concomitant change in expression levels.

We also measured expression levels of these enzymes in human patient samples of normal colonic epithelial cells and colorectal tissues. In human patient samples, we also noticed SR mRNA levels were decreased and GFRP mRNA levels were increased. QDPR and GCH-1 were not significantly altered. If we assume decreased expression of SR and increased GFRP protein levels, this would lead to an increase of BH2 in tumor cells. Future studies must be done to corroborate this finding using western blot to see protein expression changes in tumors from patients.

Using LNNA, gp91 NOX inhibitor and EUK134 (SOD mimetic) we were able to raise BH4:BH2 slightly as compared to untreated colorectal cancer cells. When we combined all three molecules, we saw the greatest increase in ratio from 2.3, to about 3.1. Although this a slight increase, it does demonstrate that the oxidative environment plays a role in diminishing BH4 levels. There are other sources of ROS/RNS within the

cells such as mitochondria, which when inhibited may contribute to increasing the BH4:BH2 ratio. We plan on developing ρ-HCT-116 cells (lacking functioning mitochondria) to determine the impact of mitochondrial ROS/RNS generation on BH4:BH2 ratio.

Our current data shows that alteration of biopterin metabolizing enzymes and ROS/RNS generating pathways play a role in decreasing the BH4:BH2 in these cancer cells. Perhaps the initial infiltration from inflammatory cells, which produce large amounts of ROS/RNS lead to a dramatic drop in BH4:BH2 ratio which then activates proliferative pathways and lead to the accumulation of more mutations. Perhaps this initial drop in BH4:BH2 leads to changes in the biopterin metabolizing enzymes themselves, eventually leading to a more permanent drop in BH4:BH2 ratio. The activation of oxidative signaling pathways as shown in chapter 2, are clearly advantageous to tumor cells, thus selected for to advance growth and progression. Earlier work in our lab using the CAC tumor model, demonstrated when SP was given to animals from the start of AOM/DSS cycles, there was decreased tumor burden in the animals. Thus a coupled NOS decreased tumor initiation in this model. However, like most monotherapies, tumor cells can find a way around them and adapt. Thus our future plans with sepiapterin are to combine with other chemotherapeutic drugs and ionizing radiation in order to determine if SP can increase efficacy of traditional cancer therapies.

Chapter 4:

Perspectives and Future Directions

Through the course of this dissertation, we have shown both *in vitro* and *in vivo* that SP leads to an increase in BH4:BH2 ratio and a decrease in proliferative pathways in colorectal tumor cells. We have also sought to explain the mechanism by which tumor cells sustain a decrease in the BH4:BH2 ratio. Although SP is able to decrease tumor size and activity *in vivo*, monotherapies are not the best tools in combating cancer. Preliminary studies in our lab have shown that SP can be combined with radiation to increase tumor cell killing.

Using Nitric Oxide, BH4 or SP as Cancer Therapeutics

A major goal of these studies was to confirm SP (by recoupling NOS and increasing NO levels) has anti-tumor effects. As mentioned earlier, NO and NOS has been shown to play a role in both tumor initiation and progression. In our own lab, we have shown L-NNA, an inhibitor of NOS, has anti-tumor effects when combined with radiation [81]. We believe that since the coupling state of NOS determines whether NO or detrimental ROS/RNS are produced, therapeutic effects of NOS inhibition, NO donors, or SP must be considered the coupling state of NOS in mind. In many cases, NO donors or NO donors combined with NSAIDs have been shown to have anti-tumor effects. NO-ASA was shown to be an effective releaser of NO and treatment of HCT116 and HT-29 colon cancer cells resulted in inhibition of growth [82]. The results showed that the NO released modified a number of cell signaling members key in tumor cell

signaling, including NFκB, β-catenin and p53, all of which were shown to be S-nitrosylated [82, 85, 104, 105]. The NO donating prodrug, O^2-(2,4-dintrophenyl) 1-[(4-ethoxycarbonyl)piperazin-1-yl]diazen-1-ium-1,2-diolate (JS-K) is another NO donating compound that has shown promise as an anti-oncogenic agent in leukemia, renal, prostate and brain cancer cells [106, 107]. Thus if an uncoupled NOS is inhibited, as in our study with L-NNA, this causes tumor cell killing. Also if the NO concentration in the tumor cells is increased where some proteins in proliferative pathways are S-nitrosylated, e.g. NFκB, this will lead to inhibition of growth and cell death.

An important caveat to using NO or SP as a potential therapeutic is the effect on tumor vascular effects of these molecules. NO and eNOS expression has been shown to increase VEGF and HIF-1 expression [108, 109]. NO can also lead to increased COX-2 expression leading to increased vascular permeability and increased angiogenesis [84]. The combination of these may increase vasculogenesis/angiogenesis in the tumor, which potentially can increase tumor growth. Thus NO or SP should not be used as a monotherapy. However this increased vascularity should increase tumor reoxygenation, which when combined with radiation, should increase tumor cell killing. The same argument applies to anti-tumor drugs, increased vascularity as a result of SP treatment also enhances drug delivery to the tumor. Importantly, SP treatment while significantly increasing BH4:BH2 in tumors is unlikely to have any significant effect on the already high BH4:BH2 in normal tissues.

Tumor Revascularization using SP

The tumor vasculature is very disordered, leaky and maintains hypoxia, especially at the core of the tumor. Hypoxia increases radio-resistance in tumor cells. A disordered and leaky vasculature also allows for invasive cells to migrate and metastasize to distant organs. Another advantage of a disordered vasculature is decreased drug delivery. One of the reasons for a disordered vasculature has been attributed to tumor endothelial cells (TECs) which are distinct from normal endothelial cells. TECs have been shown to have increased doubling times, larger nuclei, display aneuploidy, increased responsiveness to growth factors, more motile and invasive compared with normal endothelial cells. TECs have also been shown to be activated after radiation to increase pro-survival pathways such as STAT3 and PKCε. Thus we believe that TECs can increase radio-resistance of tumors. In our lab we used 2H11 mouse TECs to study the effects of SP after radiation in these cells. Figure 4.1 shows STAT3 and PKCε activation of IR in 2H11 cells. We believe the activation of these and other pro-inflammatory pathways increases radio-resistance of their adjacent tumor cells. We have also seen that radiation activates STAT3 in A549 and HCT-116 cells. Figure 4.2 shows SP treatment with IR decreases the activation of STAT3 in 2H11 cells. We also used confocal imaging to analyze for stress fiber formation (a marker for endothelial cell activation) after radiation. Figure 4.3 shows that IR increases stress fiber formation, but SP treatment decreases the formation of stress fibers. Lastly, we examined migration of 2H11 cells after radiation. Figure 4.4 shows that after IR, 2H11

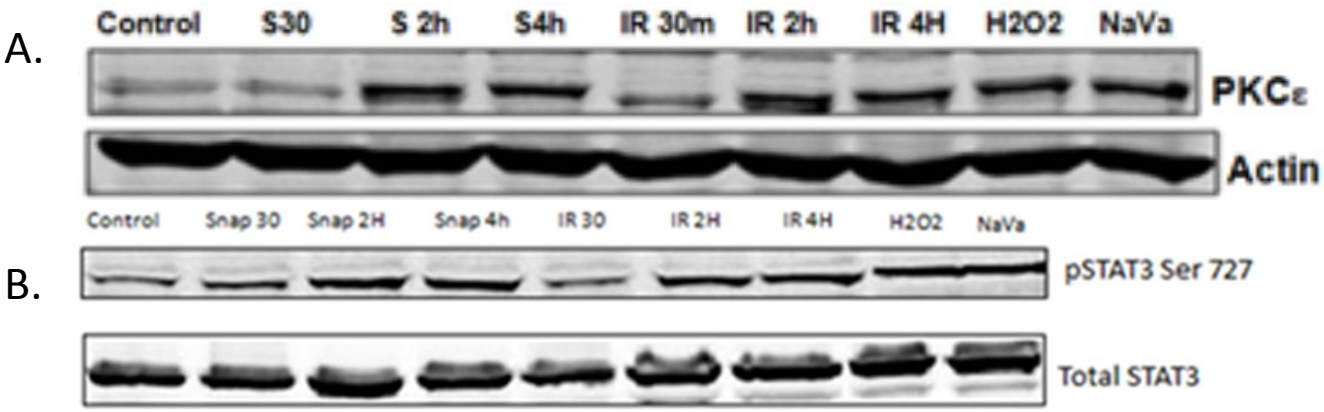

Figure 4.1 Ionizing Radiation Activates Survival Molecules in 2H11 TECs. 2H11 TEC were treated with 5 Gray IR and analyzed for increase in proliferative markers (A) PKCε and (B) STAT3 Serine 727 phosphorylation. S-Nitroso-N-Acetyl-D,L-Penicillamine (SNAP) NO donor was used as a positive control.

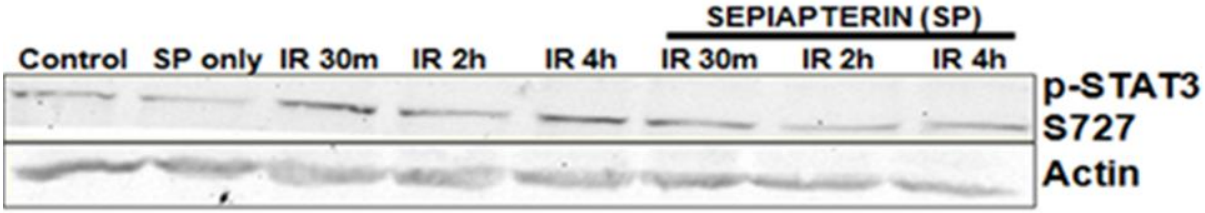

Figure 4.2: SP Treatment of 2H11 TECs before IR Decresed STAT3 Phosphorylation. 2H11 TECs were treated with 20uM SP for 24 hours, then irradiated at 5 Gray. STAT3 Serine 727 was decreased with SP treatment.

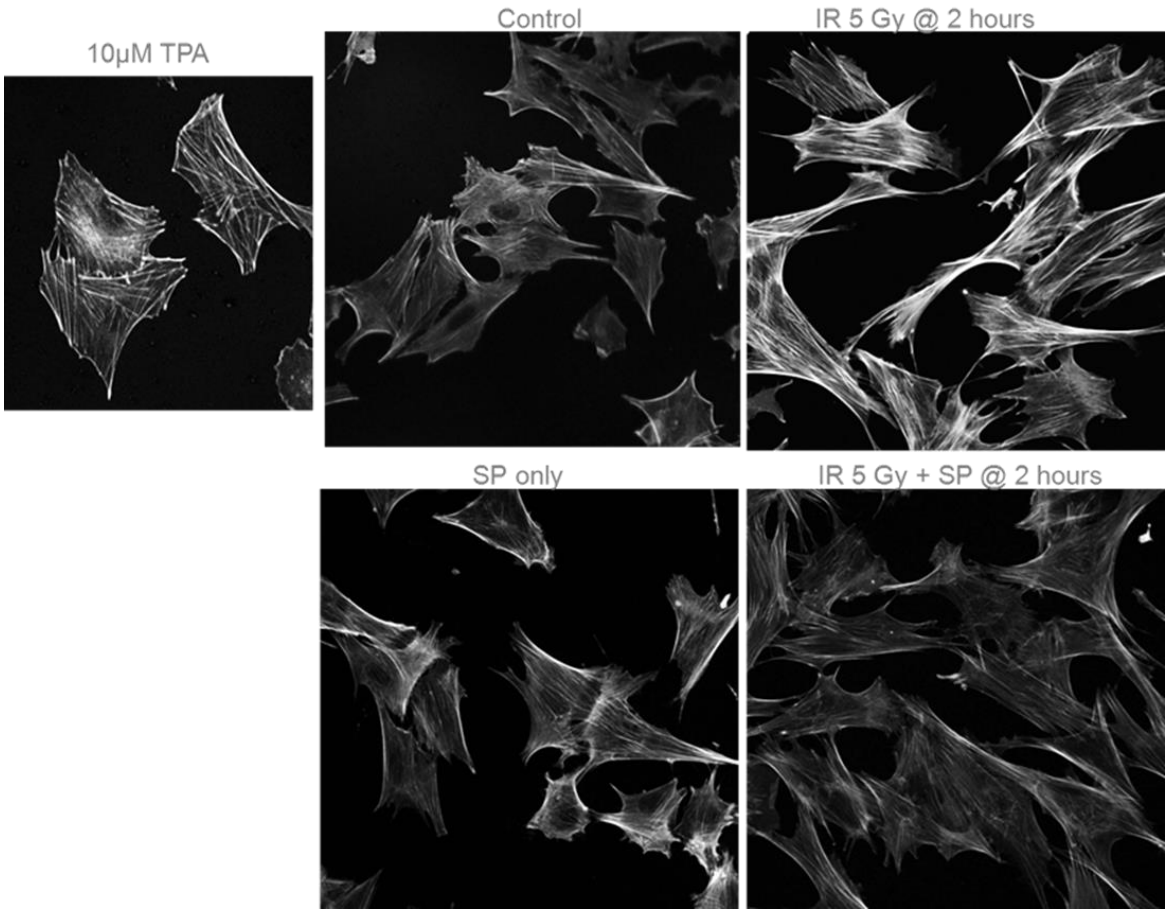

Figure 4.3: Stress Fiber Formation after IR. 2H11 TECs were treated with 5 Gray IR, and/or 20uM of SP for 24 hours. Stress fiber formation was assessed using staining for Acin-F and imaged using confocal microscopy. Phorbol ester (TPA) was used as a positive control. SP pre-treatment decreased the formation of stress fibers after IR.

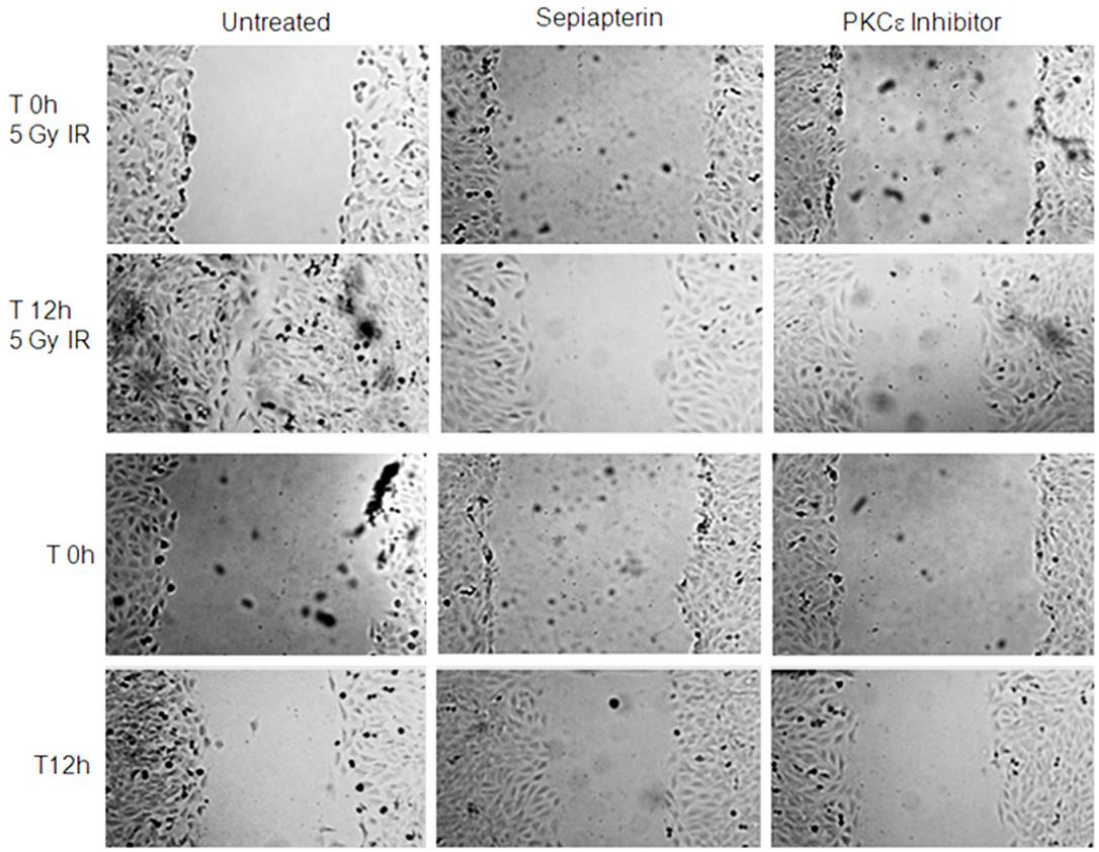

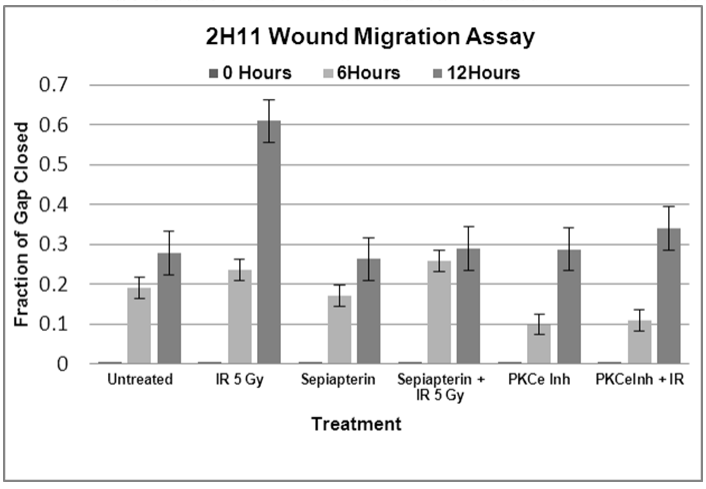

Figure 4.4: Migration Assay after IR Treatment. 2H11 TECs were grown to near confluence, then irradiated at 5 Gray. At 12 hours, untreated cells nearly closed 70% of gap, whereas 20uM SP treated cells, or cells with 10uM PKCε Inhibitor only closed about 30% of gap.

cells increased motility, however using SP, we were able to decrease the migration of these cells. Thus for this reason, we believe SP is able to decrease 2H11 activation, especially after IR. SP may be able to normalize the tumor vasculature. Other studies in our lab have shown that SP was able to increase CD31 positive cells (marker for endothelial cells) and increase oxygenated hemoglobin in both xenograft and spontaneous breast tumors. The importance of increased vascularization and oxygenation can increase radiosensitivity of the tumor as well as increase delivery of chemotherapeutic drugs. Current studies are underway to combine radiation and SP in both animals and *in vitro* cultures to determine if there is increased cytotoxicity when SP and IR are combined.

Comparisons of Human Biopsy Samples for Biopterin Metabolizing Enzymes

Although we saw mRNA differences between normal colonic epithelial cells and tumor cells in biopterin metabolizing enzymes, these data did not correlate well with protein expression or when compared with human colorectal samples. We believe this may be partly due to the CAC model we used. Due to the heterogeneity in size and stage of tumors, it may be difficult to ascertain differences. Thus plans for future studies include using biopsy material from human patients and a variety of tumor tissue and their normal tissue counterparts. We will also analyze biopterin metabolizing enzymes in MMTV Neu mice, which develop spontaneous breast tumors, to see if our results are generalizable in other tumor types. Lastly, we will see if by normalizing altered proteins in tumors, such as overexpressing SR or downregulating GFRP, can increase the BH4:BH2 *in vitro* in different tumor cells. These studies will elucidate further how tumor cells maintain a decreased BH4:BH2 ratio.

Literature Cited

1. Siegel, R.L., K.D. Miller, and A. Jemal, *Cancer statistics, 2015.* CA Cancer J Clin, 2015. **65**(1): p. 5-29.
2. Eddy, D.M., *Screening for colorectal cancer.* Ann Intern Med, 1990. **113**(5): p. 373-84.
3. Chan, A.T. and E.L. Giovannucci, *Primary prevention of colorectal cancer.* Gastroenterology, 2010. **138**(6): p. 2029-2043 e10.
4. Ponz de Leon, M., et al., *Identification of hereditary nonpolyposis colorectal cancer in the general population. The 6-year experience of a population-based registry.* Cancer, 1993. **71**(11): p. 3493-501.
5. Burt, R.W., J.A. DiSario, and L. Cannon-Albright, *Genetics of colon cancer: impact of inheritance on colon cancer risk.* Annu Rev Med, 1995. **46**: p. 371-9.
6. Lynch, H.T., et al., *Genetics, natural history, tumor spectrum, and pathology of hereditary nonpolyposis colorectal cancer: an updated review.* Gastroenterology, 1993. **104**(5): p. 1535-49.
7. Taketo, M.M. and W. Edelmann, *Mouse models of colon cancer.* Gastroenterology, 2009. **136**(3): p. 780-98.
8. MacDonald, B.T., K. Tamai, and X. He, *Wnt/beta-catenin signaling: components, mechanisms, and diseases.* Dev Cell, 2009. **17**(1): p. 9-26.
9. Beerenwinkel, N., et al., *Genetic progression and the waiting time to cancer.* PLoS Comput Biol, 2007. **3**(11): p. e225.
10. Fearon, E.R. and B. Vogelstein, *A genetic model for colorectal tumorigenesis.* Cell, 1990. **61**(5): p. 759-67.
11. Kinzler, K.W. and B. Vogelstein, *Lessons from hereditary colorectal cancer.* Cell, 1996. **87**(2): p. 159-70.
12. Vogelstein, B., et al., *Genetic alterations during colorectal-tumor development.* N Engl J Med, 1988. **319**(9): p. 525-32.
13. Biswas, S., et al., *Transforming growth factor beta receptor type II inactivation promotes the establishment and progression of colon cancer.* Cancer Res, 2004. **64**(14): p. 4687-92.
14. Papageorgis, P., et al., *Smad4 inactivation promotes malignancy and drug resistance of colon cancer.* Cancer Res, 2011. **71**(3): p. 998-1008.
15. Rodrigues, N.R., et al., *p53 mutations in colorectal cancer.* Proc Natl Acad Sci U S A, 1990. **87**(19): p. 7555-9.
16. Fleming, N.I., et al., *SMAD2, SMAD3 and SMAD4 mutations in colorectal cancer.* Cancer Res, 2013. **73**(2): p. 725-35.
17. Li, F., et al., *TGF-beta signaling in colon cancer cells.* World J Surg, 2005. **29**(3): p. 306-11.
18. Moon, R.T., et al., *WNT and beta-catenin signalling: diseases and therapies.* Nat Rev Genet, 2004. **5**(9): p. 691-701.
19. Terzic, J., et al., *Inflammation and colon cancer.* Gastroenterology, 2010. **138**(6): p. 2101-2114 e5.
20. Feagins, L.A., R.F. Souza, and S.J. Spechler, *Carcinogenesis in IBD: potential targets for the prevention of colorectal cancer.* Nat Rev Gastroenterol Hepatol, 2009. **6**(5): p. 297-305.
21. Goel, G.A., et al., *Molecular pathways underlying IBD-associated colorectal neoplasia: therapeutic implications.* Am J Gastroenterol, 2011. **106**(4): p. 719-30.
22. Lakatos, P.L. and L. Lakatos, *Risk for colorectal cancer in ulcerative colitis: changes, causes and management strategies.* World J Gastroenterol, 2008. **14**(25): p. 3937-47.
23. Sheng, H., et al., *Nuclear translocation of beta-catenin in hereditary and carcinogen-induced intestinal adenomas.* Carcinogenesis, 1998. **19**(4): p. 543-9.

24. Tuohy, T.M., et al., *Risk of colorectal cancer and adenomas in the families of patients with adenomas: a population-based study in Utah.* Cancer, 2014. **120**(1): p. 35-42.
25. Friis, S., et al., *Low-Dose Aspirin or Nonsteroidal Anti-inflammatory Drug Use and Colorectal Cancer Risk: A Population-Based, Case-Control Study.* Ann Intern Med, 2015. **163**(5): p. 347-55.
26. Piazuelo, E. and A. Lanas, *NSAIDS and gastrointestinal cancer.* Prostaglandins Other Lipid Mediat, 2015. **120**: p. 91-6.
27. Soh, J.W. and I.B. Weinstein, *Role of COX-independent targets of NSAIDs and related compounds in cancer prevention and treatment.* Progress in experimental tumor research, 2003. **37**: p. 261-85.
28. Corvinus, F.M., et al., *Persistent STAT3 activation in colon cancer is associated with enhanced cell proliferation and tumor growth.* Neoplasia, 2005. **7**(6): p. 545-55.
29. Sakamoto, K., et al., *Constitutive NF-kappaB activation in colorectal carcinoma plays a key role in angiogenesis, promoting tumor growth.* Clin Cancer Res, 2009. **15**(7): p. 2248-58.
30. Keerthivasan, S., et al., *beta-Catenin promotes colitis and colon cancer through imprinting of proinflammatory properties in T cells.* Sci Transl Med, 2014. **6**(225): p. 225ra28.
31. Oguma, K., et al., *Activated macrophages promote Wnt signalling through tumour necrosis factor-alpha in gastric tumour cells.* EMBO J, 2008. **27**(12): p. 1671-81.
32. Oguma, K., H. Oshima, and M. Oshima, *Inflammation, tumor necrosis factor and Wnt promotion in gastric cancer development.* Future Oncol, 2010. **6**(4): p. 515-26.
33. Kaler, P., L. Augenlicht, and L. Klampfer, *Macrophage-derived IL-1beta stimulates Wnt signaling and growth of colon cancer cells: a crosstalk interrupted by vitamin D3.* Oncogene, 2009. **28**(44): p. 3892-902.
34. Andrew, P.J. and B. Mayer, *Enzymatic function of nitric oxide synthases.* Cardiovascular research, 1999. **43**(3): p. 521-31.
35. Knowles, R.G. and S. Moncada, *Nitric oxide synthases in mammals.* The Biochemical journal, 1994. **298 (Pt 2)**: p. 249-58.
36. XU, W., et al., *The role of nitric oxide in cancer.*
37. Broholm, H., et al., *Nitric oxide synthase expression and enzymatic activity in human brain tumors.* Clin Neuropathol, 2003. **22**(6): p. 273-81.
38. Cianchi, F., et al., *Inducible nitric oxide synthase expression in human colorectal cancer: correlation with tumor angiogenesis.* Am J Pathol, 2003. **162**(3): p. 793-801.
39. Drew, B. and C. Leeuwenburgh, *Aging and the role of reactive nitrogen species.* Annals of the New York Academy of Sciences, 2002. **959**: p. 66-81.
40. Nathan, C., *Role of iNOS in human host defense.* Science, 2006. **312**(5782): p. 1874-5; author reply 1874-5.
41. Coggins, M.P. and K.D. Bloch, *Nitric oxide in the pulmonary vasculature.* Arteriosclerosis, thrombosis, and vascular biology, 2007. **27**(9): p. 1877-85.
42. Rabender, C.S., et al., *The Role of Nitric Oxide Synthase Uncoupling in Tumor Progression.* Mol Cancer Res, 2015. **13**(6): p. 1034-43.
43. Browning, D.D., I.K. Kwon, and R. Wang, *cGMP-dependent protein kinases as potential targets for colon cancer prevention and treatment.* Future Med Chem, 2010. **2**(1): p. 65-80.
44. Kwon, I.K., et al., *PKG inhibits TCF signaling in colon cancer cells by blocking beta-catenin expression and activating FOXO4.* Oncogene, 2010. **29**(23): p. 3423-34.
45. Lim, K.H., et al., *Tumour maintenance is mediated by eNOS.* Nature, 2008. **452**(7187): p. 646-9.
46. Vakkala, M., P. Paakko, and Y. Soini, *eNOS expression is associated with the estrogen and progesterone receptor status in invasive breast carcinoma.* Int J Oncol, 2000. **17**(4): p. 667-71.

47. Alp, N.J. and K.M. Channon, *Regulation of endothelial nitric oxide synthase by tetrahydrobiopterin in vascular disease.* Arteriosclerosis, thrombosis, and vascular biology, 2004. **24**(3): p. 413-20.
48. Antoniades, C., et al., *Induction of vascular GTP-cyclohydrolase I and endogenous tetrahydrobiopterin synthesis protect against inflammation-induced endothelial dysfunction in human atherosclerosis.* Circulation, 2011. **124**(17): p. 1860-70.
49. Cosentino, F., et al., *Chronic treatment with tetrahydrobiopterin reverses endothelial dysfunction and oxidative stress in hypercholesterolaemia.* Heart, 2008. **94**(4): p. 487-92.
50. Karbach, S., et al., *eNOS uncoupling in cardiovascular diseases--the role of oxidative stress and inflammation.* Curr Pharm Des, 2014. **20**(22): p. 3579-94.
51. Guzik, T.J., et al., *Mechanisms of increased vascular superoxide production in human diabetes mellitus: role of NAD(P)H oxidase and endothelial nitric oxide synthase.* Circulation, 2002. **105**(14): p. 1656-62.
52. Tabit, C.E., et al., *Endothelial dysfunction in diabetes mellitus: molecular mechanisms and clinical implications.* Rev Endocr Metab Disord, 2010. **11**(1): p. 61-74.
53. Cardnell, R.J., et al., *Sepiapterin ameliorates chemically induced murine colitis and azoxymethane-induced colon cancer.* J Pharmacol Exp Ther, 2013. **347**(1): p. 117-25.
54. Leslie, N.R., *The redox regulation of PI 3-kinase-dependent signaling.* Antioxid Redox Signal, 2006. **8**(9-10): p. 1765-74.
55. Murillo-Carretero, M., et al., *S-Nitrosylation of the epidermal growth factor receptor: a regulatory mechanism of receptor tyrosine kinase activity.* Free Radic Biol Med, 2009. **46**(4): p. 471-9.
56. Yakovlev, V.A., et al., *Tyrosine nitration of IkappaBalpha: a novel mechanism for NF-kappaB activation.* Biochemistry, 2007. **46**(42): p. 11671-83.
57. Zhang, Y. and J.H. Yang, *Activation of the PI3K/Akt pathway by oxidative stress mediates high glucose-induced increase of adipogenic differentiation in primary rat osteoblasts.* J Cell Biochem, 2013. **114**(11): p. 2595-602.
58. Switzer, C.H., et al., *S-nitrosylation of EGFR and Src activates an oncogenic signaling network in human basal-like breast cancer.* Mol Cancer Res, 2012. **10**(9): p. 1203-15.
59. Irani, K., et al., *Mitogenic signaling mediated by oxidants in Ras-transformed fibroblasts.* Science, 1997. **275**(5306): p. 1649-52.
60. Beckman, J.S. and W.H. Koppenol, *Nitric oxide, superoxide, and peroxynitrite: the good, the bad, and ugly.* The American journal of physiology, 1996. **271**(5 Pt 1): p. C1424-37.
61. Yakovlev, V.A. and R.B. Mikkelsen, *Protein tyrosine nitration in cellular signal transduction pathways.* J Recept Signal Transduct Res, 2010. **30**(6): p. 420-9.
62. Rafikov, R., et al., *Asymmetric dimethylarginine induces endothelial nitric-oxide synthase mitochondrial redistribution through the nitration-mediated activation of Akt1.* J Biol Chem, 2013. **288**(9): p. 6212-26.
63. Abello, N., et al., *Protein tyrosine nitration: selectivity, physicochemical and biological consequences, denitration, and proteomics methods for the identification of tyrosine-nitrated proteins.* Journal of proteome research, 2009. **8**(7): p. 3222-38.
64. Yakovlev, V.A., et al., *Nitration of the tumor suppressor protein p53 at tyrosine 327 promotes p53 oligomerization and activation.* Biochemistry, 2010. **49**(25): p. 5331-9.
65. Jaffrey, S.R., et al., *Protein S-nitrosylation: a physiological signal for neuronal nitric oxide.* Nature cell biology, 2001. **3**(2): p. 193-7.
66. Hess, D.T., et al., *Protein S-nitrosylation: purview and parameters.* Nature reviews. Molecular cell biology, 2005. **6**(2): p. 150-66.

67. Yakovlev, V.A., *Nitric oxide-dependent downregulation of BRCA1 expression promotes genetic instability.* Cancer research, 2013. **73**(2): p. 706-15.
68. Yasukawa, T., et al., *S-nitrosylation-dependent inactivation of Akt/protein kinase B in insulin resistance.* J Biol Chem, 2005. **280**(9): p. 7511-8.
69. Numajiri, N., et al., *On-off system for PI3-kinase-Akt signaling through S-nitrosylation of phosphatase with sequence homology to tensin (PTEN).* Proc Natl Acad Sci U S A, 2011. **108**(25): p. 10349-54.
70. Meng, T.C., T. Fukada, and N.K. Tonks, *Reversible oxidation and inactivation of protein tyrosine phosphatases in vivo.* Molecular cell, 2002. **9**(2): p. 387-99.
71. Barrett, D.M., et al., *Inhibition of protein-tyrosine phosphatases by mild oxidative stresses is dependent on S-nitrosylation.* The Journal of biological chemistry, 2005. **280**(15): p. 14453-61.
72. Sturla, L.M., et al., *Requirement of Tyr-992 and Tyr-1173 in phosphorylation of the epidermal growth factor receptor by ionizing radiation and modulation by SHP2.* The Journal of biological chemistry, 2005. **280**(15): p. 14597-604.
73. Kim, J.E. and S.R. Tannenbaum, *S-Nitrosation regulates the activation of endogenous procaspase-9 in HT-29 human colon carcinoma cells.* The Journal of biological chemistry, 2004. **279**(11): p. 9758-64.
74. Kim, Y.M., et al., *Nitric oxide prevents tumor necrosis factor alpha-induced rat hepatocyte apoptosis by the interruption of mitochondrial apoptotic signaling through S-nitrosylation of caspase-8.* Hepatology, 2000. **32**(4 Pt 1): p. 770-8.
75. Torok, N.J., et al., *Nitric oxide inhibits apoptosis downstream of cytochrome C release by nitrosylating caspase 9.* Cancer research, 2002. **62**(6): p. 1648-53.
76. Li, N., et al., *Sulindac selectively inhibits colon tumor cell growth by activating the cGMP/PKG pathway to suppress Wnt/beta-catenin signaling.* Mol Cancer Ther, 2013. **12**(9): p. 1848-59.
77. Thompson, W.J., et al., *Exisulind induction of apoptosis involves guanosine 3',5'-cyclic monophosphate phosphodiesterase inhibition, protein kinase G activation, and attenuated beta-catenin.* Cancer research, 2000. **60**(13): p. 3338-42.
78. Zhu, B., et al., *Suppression of cyclic GMP-specific phosphodiesterase 5 promotes apoptosis and inhibits growth in HT29 cells.* Journal of cellular biochemistry, 2005. **94**(2): p. 336-50.
79. Hausladen, A., A.J. Gow, and J.S. Stamler, *Nitrosative stress: metabolic pathway involving the flavohemoglobin.* Proceedings of the National Academy of Sciences of the United States of America, 1998. **95**(24): p. 14100-5.
80. Stamler, J.S. and A. Hausladen, *Oxidative modifications in nitrosative stress.* Nature structural biology, 1998. **5**(4): p. 247-9.
81. Cardnell, R.J. and R.B. Mikkelsen, *Nitric oxide synthase inhibition enhances the antitumor effect of radiation in the treatment of squamous carcinoma xenografts.* PloS one, 2011. **6**(5): p. e20147.
82. Gao, L. and J.L. Williams, *Nitric oxide-donating aspirin induces G2/M phase cell cycle arrest in human cancer cells by regulating phase transition proteins.* International journal of oncology, 2012. **41**(1): p. 325-30.
83. Kurimoto, M., et al., *Growth inhibition and radiosensitization of cultured glioma cells by nitric oxide generating agents.* Journal of neuro-oncology, 1999. **42**(1): p. 35-44.
84. Mollace, V., et al., *Modulation of prostaglandin biosynthesis by nitric oxide and nitric oxide donors.* Pharmacological reviews, 2005. **57**(2): p. 217-52.
85. Ouyang, N., J.L. Williams, and B. Rigas, *NO-donating aspirin inhibits angiogenesis by suppressing VEGF expression in HT-29 human colon cancer mouse xenografts.* Carcinogenesis, 2008. **29**(9): p. 1794-8.

86. Edwards, P., et al., *Tumor cell nitric oxide inhibits cell growth in vitro, but stimulates tumorigenesis and experimental lung metastasis in vivo.* J Surg Res, 1996. **63**(1): p. 49-52.
87. Franchi, A., et al., *Inducible nitric oxide synthase expression in laryngeal neoplasia: correlation with angiogenesis.* Head Neck, 2002. **24**(1): p. 16-23.
88. Gallo, O., et al., *Role of nitric oxide in angiogenesis and tumor progression in head and neck cancer.* Journal of the National Cancer Institute, 1998. **90**(8): p. 587-96.
89. Lopez-Rivera, E., et al., *Inducible nitric oxide synthase drives mTOR pathway activation and proliferation of human melanoma by reversible nitrosylation of TSC2.* Cancer Res, 2014. **74**(4): p. 1067-78.
90. Thomsen, L.L., et al., *Nitric oxide synthase activity in human gynecological cancer.* Cancer Res, 1994. **54**(5): p. 1352-4.
91. Neufert, C., C. Becker, and M.F. Neurath, *An inducible mouse model of colon carcinogenesis for the analysis of sporadic and inflammation-driven tumor progression.* Nat Protoc, 2007. **2**(8): p. 1998-2004.
92. Chowdhury, F.U., et al., *[18F]FDG PET/CT imaging of colorectal cancer: a pictorial review.* Postgrad Med J, 2010. **86**(1013): p. 174-82.
93. Nik, A.M. and P. Carlsson, *Separation of intact intestinal epithelium from mesenchyme.* Biotechniques, 2013. **55**(1): p. 42-4.
94. Landmesser, U., et al., *Oxidation of tetrahydrobiopterin leads to uncoupling of endothelial cell nitric oxide synthase in hypertension.* The Journal of clinical investigation, 2003. **111**(8): p. 1201-9.
95. Bedard, K. and K.H. Krause, *The NOX family of ROS-generating NADPH oxidases: physiology and pathophysiology.* Physiological reviews, 2007. **87**(1): p. 245-313.
96. Crabtree, M.J., et al., *Critical role for tetrahydrobiopterin recycling by dihydrofolate reductase in regulation of endothelial nitric-oxide synthase coupling: relative importance of the de novo biopterin synthesis versus salvage pathways.* J Biol Chem, 2009. **284**(41): p. 28128-36.
97. Coughlin, C.R., 2nd, et al., *Dihydropteridine reductase deficiency and treatment with tetrahydrobiopterin: a case report.* JIMD Rep, 2013. **10**: p. 53-6.
98. Hasse, S., et al., *Perturbed 6-tetrahydrobiopterin recycling via decreased dihydropteridine reductase in vitiligo: more evidence for H2O2 stress.* J Invest Dermatol, 2004. **122**(2): p. 307-13.
99. Sanchez-Urretia, L., C.E. Pierce, and O. Greengard, *Dihydropteridine reductase activity of adult, fetal and neoplastic tissues.* Enzyme, 1978. **23**(5): p. 346-52.
100. Shinozaki, K., et al., *Coronary endothelial dysfunction in the insulin-resistant state is linked to abnormal pteridine metabolism and vascular oxidative stress.* J Am Coll Cardiol, 2001. **38**(7): p. 1821-8.
101. Cong, L.N., et al., *Physiological role of Akt in insulin-stimulated translocation of GLUT4 in transfected rat adipose cells.* Mol Endocrinol, 1997. **11**(13): p. 1881-90.
102. Wang, Q., et al., *Protein kinase B/Akt participates in GLUT4 translocation by insulin in L6 myoblasts.* Mol Cell Biol, 1999. **19**(6): p. 4008-18.
103. Pluth, M.D., E. Tomat, and S.J. Lippard, *Biochemistry of mobile zinc and nitric oxide revealed by fluorescent sensors.* Annu Rev Biochem, 2011. **80**: p. 333-55.
104. Hibbs, J.B., Jr., et al., *Nitric oxide: a cytotoxic activated macrophage effector molecule.* Biochemical and biophysical research communications, 1988. **157**(1): p. 87-94.
105. Williams, J.L., et al., *NO-donating aspirin inhibits the activation of NF-kappaB in human cancer cell lines and Min mice.* Carcinogenesis, 2008. **29**(2): p. 390-7.
106. Shami, P.J., et al., *Antitumor activity of JS-K [O2-(2,4-dinitrophenyl) 1-[(4-ethoxycarbonyl)piperazin-1-yl]diazen-1-ium-1,2-diolate] and related O2-aryl diazeniumdiolates in vitro and in vivo.* Journal of medicinal chemistry, 2006. **49**(14): p. 4356-66.

107. Chakrapani, H., et al., *Synthesis, nitric oxide release, and anti-leukemic activity of glutathione-activated nitric oxide prodrugs: Structural analogues of PABA/NO, an anti-cancer lead compound.* Bioorganic & medicinal chemistry, 2008. **16**(5): p. 2657-64.
108. Bergers, G. and L.E. Benjamin, *Tumorigenesis and the angiogenic switch.* Nature reviews. Cancer, 2003. **3**(6): p. 401-10.
109. Ridnour, L.A., et al., *Molecular mechanisms for discrete nitric oxide levels in cancer.* Nitric oxide : biology and chemistry / official journal of the Nitric Oxide Society, 2008. **19**(2): p. 73-6.